Aerosol and Air Quality Research, 14: 453–469, 2014
Copyright © Taiwan Association for Aerosol Research
ISSN: 1680-8584 print / 2071-1409 online
doi: 10.4209/aaqr.2013.06.0186

Understanding the Reaction Mechanism of Photocatalytic Reduction of CO_2 with H_2O on TiO_2-Based Photocatalysts: A Review

Lianjun Liu, Ying Li*

Mechanical Engineering Department, University of Wisconsin-Milwaukee, 3200 N. Cramer Street, Milwaukee, WI 53211, USA

ABSTRACT

Recently, there has been an increasing interest in the research of photocatalytic reduction of CO_2 with H_2O, an innovative way to simultaneously reduce the level of CO_2 emissions and produce renewable and sustainable fuels. Titanium dioxide (TiO_2) and modified TiO_2 composites are the most widely used photocatalysts in this application; however, the reaction mechanism of CO_2 photoreduction on TiO_2 photocatalysts is still not very clear, and the reaction intermediates and product selectivity are not well understood. This review aims to summarize the recent advances in the exploration of reaction mechanism of CO_2 photoreduction with H_2O in correlation with the TiO_2 photocatalyst characteristics. Discussions are provided in the following sections: (1) CO_2 adsorption, activation and dissociation on TiO_2 photocatalyst; (2) mechanism and approaches to enhance charge transfer from photocatalyst to reactants (i.e., CO_2 and H_2O); and (3) surface intermediates, reaction pathways, and product selectivity. In each section, the effects of material properties are discussed, including TiO_2 crystal phases (e.g., anatase, rutile, brookite, or their mixtures), surface defects (e.g., oxygen vacancy and Ti^{3+}) and material modifications (e.g., incorporation of noble metal, metal oxide, and/or nonmetal species to TiO_2). Finally, perspectives on future research directions and open issues to be addressed in CO_2 photoreduction are outlined in this review paper.

Keywords: TiO_2; CO_2 photoreduction; Surface Defects; Intermediates; Reaction Mechanism.

INTRODUCTION

The emissions of greenhouse gases, particularly carbon dioxide (CO_2), could result in the global climate change and unhealthful regional air quality (Roy *et al.*, 2010). To reduce the emissions of CO_2 and to achieve a sustainable energy future, novel materials and new technologies have been developed that convert CO_2 into useful chemical compounds and fuels (Indrakanti *et al.*, 2009; Dhakshinamoorthy *et al.*, 2012; Kubacka *et al.*, 2012). Besides the methods of solar thermo-chemical conversion and electrochemical reduction of CO_2 (Dubois and Dubois, 2009; Furler *et al.*, 2012), solar-activated photocatalytic reduction of CO_2 with water at room temperature and atmospheric pressure (namely artificial photosynthesis) is attractive due to its relatively low cost (Roy *et al.*, 2010; Dhakshinamoorthy *et al.*, 2012).

Towards this artificial photosynthesis, various semiconductors photocatalysts (CdSe, ZrO_2, TiO_2, Ga_2O_3, and ZnO) are investigated (Wang *et al.*, 2010; Xi *et al.*, 2011; Ashley *et al.*, 2012; Dhakshinamoorthy *et al.*, 2012; Kubacka *et al.*, 2012; Liu *et al.*, 2012b; Fan *et al.*, 2013). Among them, TiO_2-based materials are most extensively studied for CO_2 photoreduction because of the stability, non-toxicity, and low cost of TiO_2. During the process of CO_2 photoreduction with H_2O, photo-illumination of the catalyst surface induces the generation of electron-hole (e^-–h^+) pairs in TiO_2. The excited electrons in the conduction band (CB) of TiO_2 could migrate to the surface and reduce CO_2 to solar fuels (e.g., CO, CH_4, CH_3OH, HCOOH). Meanwhile, the holes left in the valence band (VB) of TiO_2 could oxidize H_2O into oxygen. However, when H_2O is used as the reducing agent, the overall CO_2 photoreduction efficiency is typically very low.

The primary reasons for the limited efficiency of photocatalytic reduction of CO_2 with H_2O are as follows: (1) the highly unfavorable one-electron transfer to form CO_2^- that requires a very negative reduction potential of –1.9 V_{NHE}; (2) the strong oxidation power of the photoexcited holes (or OH radicals) that induce backward reactions, i.e., oxidizing the intermediates and products converted from CO_2; (3) the fast recombination rate of e^-–h^+ pairs in TiO_2; and (4) the limitation in the harvest of visible light due to the wide band-gap of TiO_2 (3.2 eV for anatase). In order to overcome the above limitations, several approaches have been attempted to modify TiO_2, including the incorporation

* Corresponding author.
Tel.: 1-414-229-3716; Fax: 1-414-229-6958
E-mail address: liying@uwm.edu

of TiO_2 with noble metals (Koci *et al.*, 2010; Li *et al.*, 2012; Wang *et al.*, 2012b) , metal oxides (Tseng *et al.*, 2002, 2004; Slamet *et al.*, 2005; Li *et al.*, 2010; Zhao *et al.*, 2012b; Liu *et al.*, 2013b), and nonmetals (Varghese *et al.*, 2009; Li *et al.*, 2012; Zhang *et al.*, 2011; Zhang *et al.*, 2012), the dispersion of TiO_2 on high surface area supports (Li *et al.*, 2010; Srinivas *et al.*, 2011; Wang *et al.*, 2011b; Zhao *et al.*, 2012b), and the control of TiO_2 with different morphologies and crystal phases (DeSario *et al.*, 2011; Jiao *et al.*, 2012a; Li *et al.*, 2008b; Liu *et al.*, 2012b).

Besides the efforts to enhance the efficiency of CO_2 photoreduction with H_2O, much attention has been paid to clarify the reaction mechanism behind this reaction. In addition to theoretical calculations (Markovits *et al.*, 1996; Pan *et al.*, 2009; He *et al.*, 2010; Indrakanti *et al.*, 2011; Pipornpong *et al.*, 2011; Rodriguez *et al.*, 2012), various microscopic (e.g., scanning tunneling microscopy (STM)) (Lee *et al.*, 2011; Sutter *et al.*, 2011) and spectroscopic (e.g., diffuse reflectance infrared Fourier transform spectroscopy (DRIFTS), electron paramagnetic resonance (EPR)) (Schilke *et al.*, 1999; Ulagappan and Frei, 2000; Wu and Huang, 2010; Dimitrijevic *et al.*, 2011; Yang *et al.*, 2011; Liu *et al.*, 2012a; Shkrob *et al.*, 2012) studies have been conducted to understand the steps associated with CO_2 adsorption, activation, and dissociation. These steps are found to be significantly affected by crystal phases (e.g., anatase, rutile), surface acidic-basic sites (e.g., hydroxyl group), defect disorders (e.g., oxygen vacancy (V_O)), co-adsorbates (e.g., H_2O), and electronic structure (e.g., charge transport) of TiO_2.

Several reviews have described the strategies and challenges in the design of TiO_2-containing photocatalysts for CO_2 photoreduction (Indrakanti *et al.*, 2009; Roy *et al.*, 2010; Dhakshinamoorthy *et al.*, 2012; Mori *et al.*, 2012). For example, Dhakshinamoorthy *et al.* (2012) summarized the photocatalytic performance of TiO_2-based photocatalysts in correlation with the catalyst structure/properties. Indrakanti *et al.* (2009) analyzed photoinduced activation of CO_2 from surface state and surface sites on metal-doped TiO_2, dye-sensitized TiO_2, defective TiO_2, and isolated-Ti in porous materials. Unfortunately, the charge transfer mechanisms in TiO_2-based materials are seldom addressed in those literature reviews. In the recent few years, some novel oxygen-deficient TiO_{2-x} materials and bicrystalline TiO_2 with controllable phase content have been applied for CO_2 photoreduction. Moreover, microscopic (e.g., STM) and spectroscopic techniques (e.g., DRIFTS, EPR) have been performed to explore the activation and dissociation mechanism of CO_2, to identify the reaction intermediates, and to probe the reaction pathways. Those new findings in the recent studies are not included in the past review papers. Hence, this review aims to summarize the recent research progress on mechanistic studies in CO_2 photoreduction in correlation with the material properties of TiO_2-based catalysts. There are three main sections in this review. The first section briefly describes CO_2 adsorption, activation and dissociation steps. The second section discusses the charge separation and transfer from TiO_2 to CO_2 and H_2O. The third section focuses on the surface intermediates and reaction pathways of CO_2 reduction. In each of the three sections, the reaction mechanism is discussed in the context of three factors including the crystal phase, defect disorders, and specific material modification of TiO_2. At the end of this review, we have summarized the research progresses and challenges and made recommendations for future research in the field of CO_2 photoreduction.

CO_2 PHOTOREDUCTION ON TIO_2-BASED MATERIALS: ACTIVATION AND DISSOCIATION

The photoreduction of CO_2 is a multistep process involving the adsorption, activation of CO_2 and dissociation of C−O bond. The adsorption of CO_2 is the initial step during the photocatalytic reaction, but the importance of this step is often neglected in the literature. Another key step is the activation of CO_2 through the transfer of photogenerated electrons from photocatalyst surface to CO_2. At the gas-solid interface, the feasibility of electron transfer from TiO_2 CB to CO_2 depends on the electron affinity of gaseous CO_2 and the interaction of CO_2 with TiO_2 surface (Indrakanti *et al.*, 2009). When CO_2 interacts with TiO_2 surface sites (e.g., Ti^{3+}) and gains electrons from TiO_2, $CO_2^{\delta-}$ species could be formed. The linear structure of CO_2 is then transformed to a bent form, where the C−O bond is likely broken (Rasko and Solymosi, 1994). Generally, the mechanism in the activation and subsequent reduction of CO_2 involves the participation of protons and electron transfer (one, two, or multiple electron process). Among them, CO_2^-, produced by one electron transfer to CO_2, is an important intermediate. In this section, one-electron induced activation and dissociation of CO_2 mechanism is discussed.

Theoretical and experimental studies consistently showed that the CO_2 adsorption, activation, and dissociation processes were significantly influenced by the crystal phase of TiO_2 and the defect disorders in TiO_2 (Pan *et al.*, 2009; He *et al.*, 2010; Liu *et al.*, 2012b; Rodriguez *et al.*, 2012). Adsorption of CO_2 on the perfect and oxygen-deficient rutile (110), anatase (101) and brookite (210) surfaces has been investigated using dispersion-corrected density functional theory (DFT) and first-principles calculations (Markovits *et al.*, 1996; Schobert *et al.*, 2008; He *et al.*, 2010; Rodriguez *et al.*, 2012). Compared with the defect-free surface, the presence of V_O on the rutile (110), anatase (101) or brookite (210) surface induced the formation of new adsorption configurations, where CO_2 was bonded at the defect sites (He *et al.*, 2010; Indrakanti *et al.*, 2011; Pipornpong *et al.*, 2011; Sutter *et al.*, 2011; Rodriguez *et al.*, 2012). Although the interactions of CO_2 with the brookite (210) surface and anatase (101) surface have similar energy, the defect-free brookite surface had negligible charge transfer to the CO_2 molecule. Once defect disorders such as V_O were created on the surface, the binding of CO_2 with brookite and anatase was favorable (Rodriguez *et al.*, 2012). Electrons stored in the V_O could be spontaneously transferred to CO_2. Once the CO_2^- radical was formed, it may decompose into CO through the occupation of one oxygen atom into the V_O site. The overall reaction is written as follows: $CO_2 + [TiO_2 + V_O] \rightarrow CO + [TiO_2]$ (Pipornpong *et al.*, 2011). In

addition, the surface V_O on anatase (101) and rutile (110) favors H_2O and O_2 adsorption and dissociation (Aschauer *et al.*, 2010). Notably, H_2O, O_2 and CO_2 molecules may compete for the same V_O sites. Since the binding energies of H_2O and O_2 molecules are 0.64 and 2.78 eV higher than that of CO_2 on the vacancy site (He *et al.*, 2010), the adsorption of CO_2 can be hindered by H_2O and O_2.

The above theoretical studies indicated that the electrons originated from the defective TiO_2 itself induced the formation of CO_2^- and the subsequent dissociation of CO_2^- to CO in the dark. This electron-induced dissociation of CO_2 was experimentally confirmed by STM study (Lee *et al.*, 2011), and the mechanism is shown in Fig. 1. The dissociation probability (P_{diss}) of CO_2 depended on the energy of the injected electrons from the STM tip. As shown in Fig. 1(A), the value of P_{diss} increased with increasing bias voltage, eventually reaching 1 at +2.2 V. In the dissociation process of CO_2, a metastable CO_2^- was formed through an electron attachment. This temporary CO_2^- can be formed only if the bias voltage is higher than V_{thres} = 1.7 eV, as shown in Fig. 1(B). Fig. 1(C) shows the scheme of CO_2 dissociation process. After a tunneling electron from the STM tip was successfully attached to CO_2, a negative CO_2^- was formed. Upon dissociation of the C–O bond, the fragment O atom of CO_2^- healed the V_O sites on the rutile (110) surface. Subsequently, the CO fragment desorbed from the surface or moved away from the reaction site.

In situ DRIFTS studies also confirmed that CO_2 could be spontaneously dissociated into CO on reduced Rh/TiO_{2-x} (Rasko and Solymosi, 1994) or defective Cu(I)/TiO_{2-x} (P25) (Liu *et al.*, 2012a) even in the dark. Fig. 2(a) shows the in situ DRIFTS spectra of CO_2 interaction with Cu(I)/TiO_{2-x} at 25°C in the dark. The exposure of the defective surface to CO_2 rapidly led to the generation of CO_2^- species (1673 and 1248 cm^{-1}) bonded with Ti^{4+}. The formation of Ti^{4+}–CO_2^- suggested that CO_2 can be activated in a way that excess electrons, being trapped at Ti^{3+}/V_O sites, migrate to adsorbed CO_2 spontaneously through a dissociative electron attachment process. Further prolong the time to 10 min resulted in the gradual decrease of CO_2^- intensity. In the meantime, a small peak at 2110 cm^{-1} assigned to CO coordinated with Cu^+ evolved, suggesting the formation of CO from the metastable CO_2^-.

To confirm this dissociation of CO_2 to CO on the defective Cu(I)/TiO_{2-x} surface, an isotopic carbon-labeling experiment was conducted under the same condition. Fig. 2(b) shows the in situ DRIFTS spectra of $^{13}CO_2$ interaction with Cu(I)/TiO_{2-x}, which follows a similar trend to that of $^{12}CO_2$ in Fig. 2(a). $^{13}CO_2^-$ species (1217 cm^{-1}) were quickly formed and then gradually decreased after reaching its maximum at 10 min. A corresponding Cu^+–^{13}CO peak at 2064 cm^{-1} appeared and reached it maximum at 10 min. The result of labeled carbon confirms that the produced CO bound to Cu^+ site is indeed derived from CO_2 and that CO_2 is indeed activated and dissociated on defective Cu(I)/TiO_{2-x}, even in the dark at room temperature.

The spontaneous dissociation of CO_2 on Rh/TiO_{2-x} and Cu(I)/TiO_{2-x} in the dark is to a large extent associated with the surface V_O that provide not only an electronic charge (Ti^{3+}) but also the sites for the adsorption of oxygen atoms from CO_2. The formation of Cu^+–CO or Rh–CO could be an additional driving force to promote the dissociation of CO_2. Furthermore, photoillumination could promote the dissociation of CO_2. Fig. 2(c) shows the in situ DRIFTS spectra acquired by sequentially exposing Cu(I)/TiO_{2-x} to CO_2 in the dark for 30 min and under photoillumination for another 30 min. After 30 min in the dark, CO_2^- at 1248 cm^{-1} and Cu^+–CO at 2110 cm^{-1} were not observed, although they

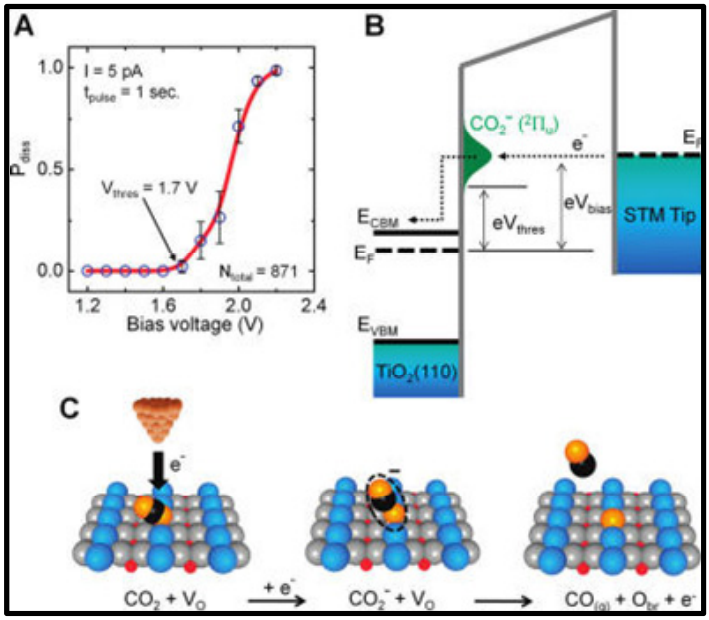

Fig. 1. (A) Dissociation probability (P_{diss}) as a function of bias voltage; (B) The electron transfer process at the STM tip/CO_2/TiO_2 interface (above V_{thres} = 1.7 eV, the electrons start to tunnel into the negative-ion state of the adsorbed CO_2); (C) Schematics of an electron induced CO_2 dissociation process. Reproduced with permission from Ref. (Lee *et al.*, 2011).

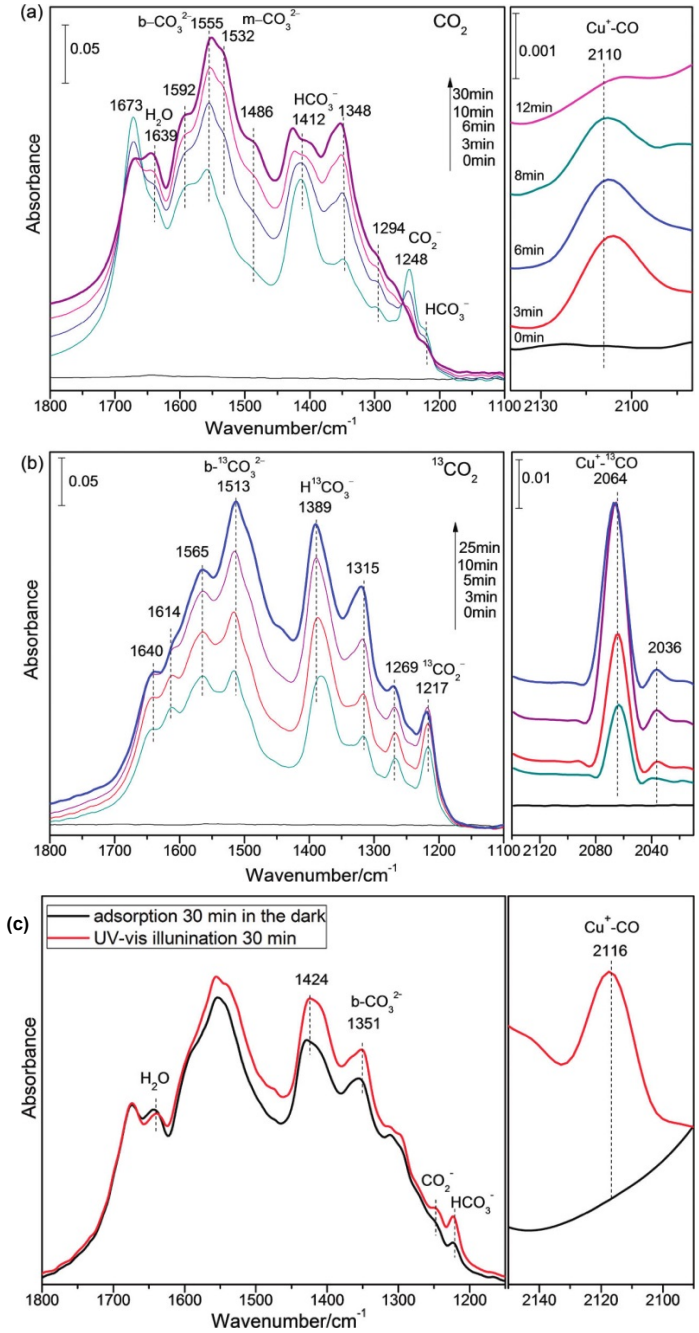

Fig. 2. In situ DRIFTS spectra of (a) CO_2 and (b) $^{13}CO_2$ interaction with defective Cu(I)/TiO_{2-x} at 25°C in the dark; (c) in situ DRIFTS spectra of CO_2 interaction with Cu(I)/TiO_{2-x} in the dark and under photoillumination subsequently. Reproduced with permission from (Liu *et al.*, 2012a).

did appear upon the exposure to CO_2 at the beginning (See Fig. 2(a)). Subsequent photoillumination induced the re-presence of CO_2^- and Cu^+–CO species. The results obtained by IR study in Fig. 2(c) suggest that photoillumination significantly promotes the activation and dissociation of CO_2.

Two possible reasons could explain the enhanced CO_2 activation and dissociation by photoillumination. First, photoillumination induced a sustained electron transfer from the catalyst to the π orbital of adsorbed CO_2. This process makes CO_2 more anionic, and thus induced the cleavage of the C–O bond (Rasko and Solymosi, 1994). Second, photoillumination could induce the regeneration of surface V_O. As illustrated in Fig. 1(c), the surface V_O is filled during the CO_2 dissociation process, which suggests the dissociation of CO_2 in the dark is likely stoichiometric rather than catalytic. However, photoillumination is capable of creating surface V_O in a way that surface oxygen atoms are oxidized to O_2 by photogenerated holes causing the formation of surface V_O (Wu and Huang, 2010). Similarly, partial regeneration of surface V_O on the Cu(I)/TiO_{2-x} catalyst may have occurred that accelerates the dissociation of CO_2 under the photoillumination (Liu *et al.*, 2012a).

CO_2 PHOTOREDUCTION ON TIO_2-BASED MATERIALS: CHARGE TRANSFER MECHANISM

For photocatalytic reduction of CO_2 with H_2O, an important step is the generation of e^-–h^+ pairs upon absorption of photons energy greater than or equal to the band gap of the photocatalyst (Dhakshinamoorthy *et al.*, 2012). However, the recombination rate of e^-–h^+ pairs is nearly two or three orders of magnitude faster than the rate of charge separation/transport (Fan *et al.*, 2013). This is a main limiting factor for the low efficiency of CO_2 conversion. Hence, any strategy that can inhibit the recombination of e^-–h^+ or facilitate the charge separation and migration from the catalyst surface to reactants will enhance the efficiency of CO_2 photoreduction. For TiO_2-based photocatalysts, the charge separation and transfer process is closely related to TiO_2 crystal phase, defect disorder in TiO_2, and material modifications to TiO_2.

Effect of Crystal Phase

TiO_2 commonly occurs in three crystalline polymorphs: rutile, anatase, and brookite. TiO_2 anatase, rutile or anatase-rutile mixed phase (e.g., Degussa P25 with a composition of 75% anatase and 25% rutile) has been frequently studied in photocatalytic reduction of CO_2, using either bare TiO_2 or with incorporation of metal, nonmetal or metal oxide species (Anpo *et al.*, 1995; Tseng *et al.*, 2004; Koci *et al.*, 2009; Zhang *et al.*, 2011; Wang *et al.*, 2012a; Wang *et al.*, 2012b). By contrast, the brookite phase or anatase-brookite mixed phase is much less studied as a photocatalyst for CO_2 photoreduction, probably due to the previous difficulty in synthesizing high quality brookite nanocrystallites. The studies on pure phase TiO_2 show that anatase phase is more photocatalytically active than rutile, possibly attributed to the combined effect of lower recombination rate of electron-hole pairs and higher surface adsorptive capacity (Hurum *et al.*, 2003; Li and Gray, 2007; He *et al.*, 2012). Recently, the much less studied brookite phase was found to have a catalytic activity similar to anatase but higher than rutile for CO_2 photoreduction with H_2O (Liu *et al.*, 2012b).

Among the studies on the mixed-phase TiO_2, anatase-rich anatase/rutile is more active than pure anatase or rutile for CO_2 photoreduction (Li *et al.*, 2008b; Wang *et al.*, 2012a). The enhanced activity of anatase/rutile mixture compared with single phase anatase or rutile was primarily attributed to the effective charge separation and transfer occurring between anatase and rutile. However, the findings in the charge transfer mechanism are not conclusive. Fig. 3 shows the two typical models of charge transfer between anatase and rutile. Some literature results (Bickley *et al.*, 1991; Kawahara *et al.*, 2002; Wang, Bai *et al.*, 2012) suggested that photogenerated electrons tend to transfer from anatase to rutile, because the conduction band (CB) of anatase is more negative than that of rutile (Fig. 3(A)). The rutile phase acts as a passive electron sink hindering charge recombination in anatase. On the contrary, Gray and co-workers used EPR spectroscopy to monitor the direction of electron migration; they proposed a mechanism that electrons migrate from the higher-level rutile CB to the lower-level anatase lattice trapping sites (Fig. 3(B)). In this case, the rutile phase serves as an antenna to extend the photoactivity into visible light range (Hurum *et al.*, 2003; Li and Gray, 2007).

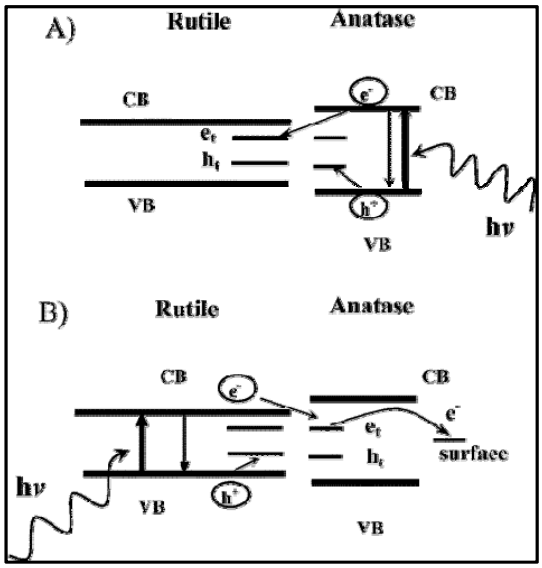

Fig. 3. (A) Previously speculated model of P25 activity where charge separation occurs on anatase and rutile acts as an electron sink. (B) Proposed model of a rutile antenna and subsequent charge separation. Reproduced with permission from (Hurum *et al.*, 2003).

Besides anatase/rutile mixtures, TiO_2 anatase/brookite mixtures have been applied for the photodegradation of organic compounds (e.g., methyl orange, rhodamine B) (Chiarello *et al.*, 2011; Boppella *et al.*, 2012; Gai *et al.*, 2012; Jiao *et al.*, 2012b; Zhao *et al.*, 2012a), which exhibited higher activity than P25 and pure-phase anatase. Recently, bicrystalline TiO_2 with controllable anatase/brookite phase content has been used as a photocatalyst for CO_2 photoreduction with H_2O (Zhao *et al.*, 2013). The activity results showed that bicrystalline anatase-brookite was generally more active than single phase anatase and brookite. Analogous to the anatase/rutile mixture, the enhanced performance of anatase/brookite was primarily attributed to the interfacial electron transfer from brookite to anatase. Among the bicrystalline anatase-brookite mixtures, the anatase-rich mixture with a composition of 75% anatase and 25% brookite showed the highest activity, and was far more active than the anatase-rutile mixture with similar anatase fraction (i.e., P25). This may be due to the following reasons: (1) brookite itself is more active than rutile as a photocatalyst (Liu *et al.*, 2012b), (2) brookite has a higher conduction band (CB) edge than rutile, which will promote the reaction of CO_2 reduction with H_2O that has a high reduction potential (Anpo *et al.*, 1995), and (3) the excited electrons on brookite CB may transfer to anatase CB due to a slightly higher CB edge of brookite than anatase.

Effect of Defect Disorders

TiO_2 is a nonstoichiometric compound, which contains defect disorders in terms of oxygen vacancies (V_O) and titanium interstitials (Nowotny *et al.*, 2008). These defects

can be created by photo-excitation in the presence of a hole scavenger (Panayotov *et al.*, 2012), thermal removal of lattice oxygen with a reducing gas (Chen *et al.*, 2011; Liu *et al.*, 2013a), doping anions such as N and C (Gai *et al.*, 2012; Hoang *et al.*, 2012; Li *et al.*, 2012), thermal treatment in vacuum (Xiong *et al.*, 2012), or plasma treating (DeSario *et al.*, 2011). The defects have been reported to play an essential role in photocatalytic degradation of organics and water splitting by TiO_2 (Chen *et al.*, 2011; Hoang *et al.*, 2012; Xing *et al.*, 2013). Three reasons can explain the importance of defects in TiO_2. First, the creation of defects could introduce intermediate surface states that narrow the band gap and hence extending the photoresponse of TiO_2 to visible light range (Chen *et al.*, 2011; DeSario *et al.*, 2011). Second, the donor state located below the TiO_2 CB promotes the charge separation and transfer (Nowotny *et al.*, 2006). Third, Ti^{3+} and V_O are considered to be important active sites for the adsorption and activation of reactants (Sutter *et al.*, 2011). Fig. 4(a) shows the charge transfer mechanism in oxygen-deficient TiO_2. Electrons could be excited from the VB to the defects donor state (red dashed line) under visible light illumination. The lifetime of electrons in the defects donor state is much longer than that on the CB (Lin *et al.*, 2005; Xing *et al.*, 2013), which facilitates the formation of superoxide radicals by attachment of electrons to oxygen. Meantime, the holes left in the VB accelerate the generation of free OH radicals. The superoxide and OH radicals are responsible for the enhanced activity of TiO_{2-x} for the photodegradation of organic compounds (Xing *et al.*, 2013).

Although oxygen-deficient TiO_{2-x} is a promising candidate as a photocatalyst, only limited work has been done for CO_2 photoreduction over TiO_{2-x}. DeDario *et al.* (2011) fabricated defective anatase/rutile thin film by direct current magnetron sputtering and applied it as a photocatalyst for CO_2 photoreduction. They demonstrated that the photocatalytic activity was influenced by the levels of oxygen deficiency in the films, which were controlled by adjusting the oxygen partial pressure during the film deposition process. They also suggested that V_O likely had two competing roles: (1) V_O could enhance visible light harvesting and act as active/adsorption sites, and (2) V_O may serve as or induce the creation of active interfacial sites at certain concentrations. Beyond that level these sites may function as recombination centers to hinder the photoactivity.

The photoactivity of defective TiO_2 was also influenced by its crystal phase (Liu *et al.*, 2012b). The CO and CH_4 production from CO_2 photoreduction was in the order of brookite, anatase and rutile. Possible reasons for this superior activity of defective brookite include the facilitated formation of V_O, faster reaction rate of CO_2^- with adsorbed H_2O or surface OH groups, and an additional reaction route involving an HCOOH intermediate (Pan *et al.*, 2009; Liu *et al.*, 2012b). It is noted that V_O, generated from thermal treatment with inert gas under the atmospheric pressure, was not stable in an air environment and was consumed during the photoreaction process (Liu *et al.*, 2012a, b). Further studies are necessary to develop more stable and more efficient TiO_{2-x} for solar fuels production, and to better understand the specific roles of defects (i.e., V_O, Ti interstitial) and the dynamics of charges separation and transfer.

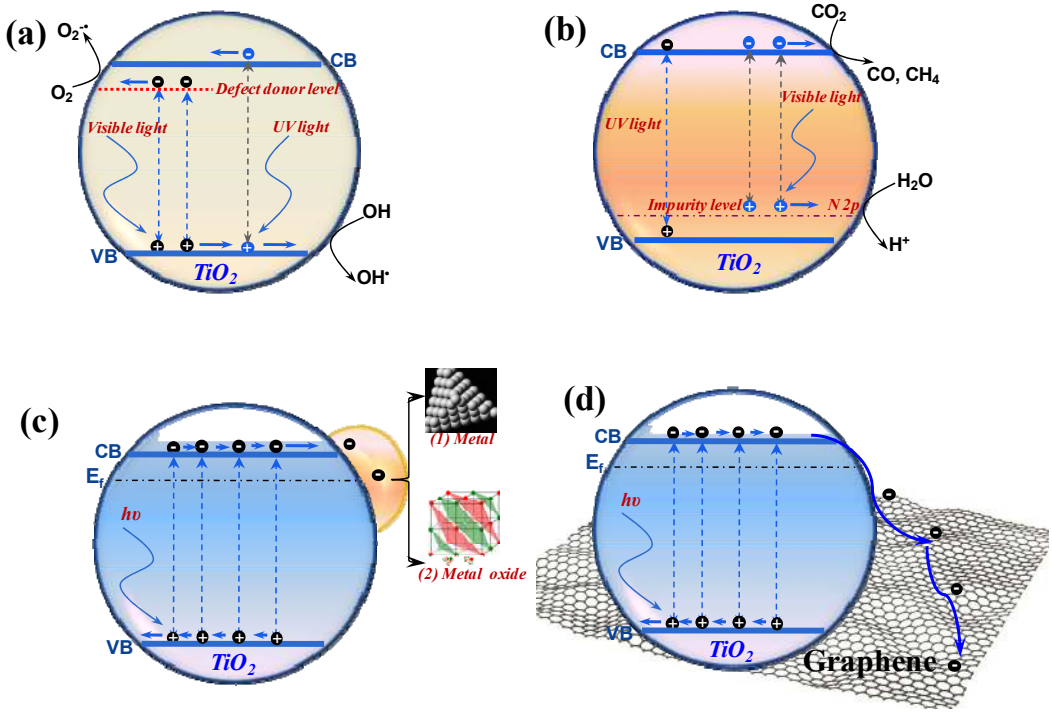

Fig. 4. Schematic illustration of charge transfer mechanism in (a) defective TiO_{2-x}, (b) N-doped TiO_2, (c) noble metals or metal oxides-modified TiO_2, and (d) graphene coupled-TiO_2. Adapted from (Liang *et al.*, 2011; Li *et al.*, 2012; Wang *et al.*, 2012b; Xing *et al.*, 2013).

Effect of Materials Modification

The discussions in sections 3.1 and 3.2 suggest that charge transfer in TiO_2 can be promoted by tailoring its phase content and engineering defect disorders on the surface. In this section, we discuss another three main strategies to enhance charge transfer by modifying TiO_2 with some other elements or species. First, doping TiO_2 with nonmetal elements (e.g., N and I) could narrow the band gap of TiO_2 and/or create impurity energy levels above the VB (Zhang *et al.*, 2011; Li *et al.*, 2012). The excited electrons by visible light are transferred from the impurity state to TiO_2 CB. Second, electron transfer could be promoted in the direction from TiO_2 CB to external trappers or carriers. The electron trappers can be noble metals (e.g., Pt, Pd, Au, Ag) (Sasirekha *et al.*, 2006; Iizuka *et al.*, 2011; Yui *et al.*, 2011; An *et al.*, 2012; Uner and Oymak, 2012; Wang *et al.*, 2012b) or metal oxides (e.g., CuO, FeO_x, CeO_2) (Tseng *et al.*, 2004; Qin *et al.*, 2011; Srinivas *et al.*, 2011; Wang *et al.*, 2011b; Truong *et al.*, 2012; Zhao *et al.*, 2012b), and the electron carriers are often carbon materials (e.g., graphene) (Liang *et al.*, 2011, 2012; Tu *et al.*, 2012). Third, the incorporation of TiO_2 with another semiconductor, i.e., photo-sensitizer (e.g., AgBr, CdSe, PbS) (Wang *et al.*, 2010; Asi *et al.*, 2011; Wang *et al.*, 2011a; An *et al.*, 2012) or n-type semiconductor (e.g., ZnO) (Xi *et al.*, 2011), promotes electron transfer between the CB of the second semiconductor and the CB of TiO_2.

Electron Transfer from the Impurity State to TiO_2 CB

The photocatalytic efficiency of TiO_2 for CO_2 photoreduction under visible light is very low due to its large band gap of 3.0–3.2 eV. It was found that doping of TiO_2 with nonmetal elements improved the visible light activity, depending on the type and the concentration of nonmetal dopants. Among the various nonmetal dopants, N-doped TiO_2 is widely used in photooxidation of organics (Lin *et al.*, 2005; Chen and Burda, 2008; Gai *et al.*, 2012) and in CO_2 photoreduction as well (Varghese *et al.*, 2009; Fan *et al.*, 2011; Zhang *et al.*, 2011; Li *et al.*, 2012; Peng *et al.*, 2012; Zhang *et al.*, 2012). However, the origin of the visible light activity of N-doped TiO_2 has long been debated. One general mechanism is shown in Fig. 4(b). Doped N gives rise to an impurity state above the TiO_2 VB. The mixing of N 2p orbital and the TiO_2 VB narrows the band gap of TiO_2 and extends the photoresponse of TiO_2 to the visible light region (Lin *et al.*, 2005; Chen and Burda, 2008; Li *et al.*, 2012). Visible light irradiation will induce the electron transfer from the nonmetal impurity state to the CB, while the photogenerated holes left in the impurity state may oxidize H_2O to O_2 or OH groups to OH• radicals. This impurity state is regarded as the highest occupied N 2p orbital. XPS analysis by Li *et al.* (2012) indicated that the oxidation state of doped N is molecularly chemisorbed N_2 or NO/NO_2 species. Similarly, Asahi *et al.* (2001) attributed the visible light sensitivity of N-doped TiO_2 to the substitutional N atoms. By contrast, Noda *et al.* (1986) concluded that the visible light activity of N-doped TiO_2 was due to V_O rather than the N impurity state. The electron transfer thus follows the mechanism illustrated in Fig. 4(a) rather than in Fig. 4(b). Other studies made similar conclusions that visible light activity of N-doped TiO_2 was ascribed to V_O which induced donor states located below the CB, while substitutional N acted as an inhibitor for e^-–h^+ recombination (Justicia *et al.*, 2002; Ihara *et al.*, 2004). This controversy makes it necessary to decouple the contributions of V_O and N-doping in TiO_2 in future studies.

Recently, a new type of visible light responsive catalyst, iodine-doped TiO_2 (I-TiO_2), has been explored for CO_2 photoreduction, and the electron transfer mechanism in I-TiO_2 is similar to that of N-TiO_2 illustrated in Fig. 4(b) (Zhang *et al.*, 2011, 2012). The iodine doping resulted in a reduced crystal size of TiO_2 and a red-shift of the TiO_2 absorption edge to the visible region. Moreover, titanium ions (i.e., Ti^{4+}) were partially substituted by iodine ions (i.e., I^{5+}) and consequently, Ti^{3+} was generated for charge balance. The Ti^{3+} sites may trap photoinduced electrons and inhibit charge recombination, which is an advantage of the iodine dopant over other nonmetal dopants. I-TiO_2 demonstrated significant enhancement in CO_2 photoreduction to CO compared with undoped TiO_2 under both visible light and UV-vis irradiation. The concentration of the iodine dopant could affect the visible light and UV-vis light activities of I-TiO_2. For iodine doping higher than 10 wt%, the activity of I-TiO_2 under UV-vis irradiation was not superior to that seen under visible light. The formation of recombination centers at high doping levels could account for this phenomenon.

Electron Transfer from TiO_2 CB to Trapping Sites

Fig. 4(c) shows the electron transfer mechanism on the noble metals or metal oxides modified TiO_2. Photogenerated electrons on TiO_2 can be easily trapped by the noble metal nanoparticles, because the Fermi energy levels of noble metals are typically lower than that of TiO_2. Such separation process leads to the formation of Schottky barrier at the interface of metal-semiconductor, which can retard the recombination of e^-–h^+ pairs. The noble metal particles also sever as co-catalysts by providing active sites for the activation and dissociation of H_2O and CO_2. The two functions of noble metals can enhance the activity of TiO_2 towards CO_2 photoreduction. The promotional effects of noble metals on the separation and transport of carriers depend on the type, state of dispersion, particle size, and valence state of noble metals. Li *et al.* (2012) found that Pt-modified TiO_2 showed a higher activity than Au and Ag-coupled TiO_2, likely due to the higher work function of Pt (5.65 eV) than Au (5.1 eV) and Ag (4.26 eV). Wang *et al.* (2012) demonstrated that either too small or too large Pt particles exhibited lower production rate of CH_4. It was proposed that the energy for band separation of the smaller Pt particles was higher due to the quantum confinement, thus preventing electron transfer from TiO_2 CB to Pt. Yui *et al.* (2011) suggested that the addition of Pd to TO_2 induced the reduction of CO_2 to CH_4, while the oxidation of Pd to PdO caused the catalyst deactivation. The above studies indicate the importance of choosing an appropriate noble metal, tailoring the particle size in an appropriate range, and avoiding the oxidation of noble metal to metal oxide.

For transition metal oxides modified TiO_2 composites

(Fig. 4(c)), the most popular photocatalyst is probably CuO_x/TiO_2, where CuO_x indicates copper oxides that are either Cu_2O or CuO. Take CuO/TiO_2 as an example, light irradiation induces the photoexcited electrons transfer from TiO_2 to the dispersed CuO. The electrons trapped by CuO are consumed by reducing CO_2 into CH_4 and CO; meanwhile, the holes oxidize H_2O into O_2. To evidence the direct electron transfer between Cu^{2+} and TiO_2, X-ray photoelectron spectroscopy (XPS) and X-ray absorption fine structure (XAFS) were employed to identify the chemical state and environment of Cu^{2+} before and after irradiation (Irie *et al.*, 2009). The results demonstrated that for Cu^{2+}-grafted TiO_2, Cu^{2+} was incorporated in a distorted amorphous CuO-like structure, which could form clusters and attach to TiO_2 surface. Photoinduced electrons were directly transferred from TiO_2 to Cu^{2+} that led to the formation of Cu^+, while the produced Cu^+ could be oxidized back to Cu^{2+} by O_2.

The enhanced charge separation by CuO_x is greatly influenced by its concentration, dispersion, and valence state. The addition of too high a concentration of CuO_x beyond the optimum value would lead to decreased photocatalytic efficiency. It is possibly because of (1) the shading effect of CuO_x that reduces the light absorption of TiO_2 and (2) CuO_x acting as charge recombination centers at high concentrations (Li *et al.*, 2008a; Irie *et al.*, 2009).

The effect of Cu valence in CuO_x is still controversial. Highly dispersed surface Cu^+ species is reported to be more active than Cu^{2+} and Cu^0, probably because Cu^+ has the highest positive reduction potential value (Cu^+/Cu^0 = 0.52 V). However, Slamet *et al.* (2005) suggested that Cu^{2+} was more active than Cu^+ and Cu^0 obtained by H_2 reduction. They argued that due to the strong interaction between TiO_2 and Cu^+ implanted in the vacant sites of TiO_2, the trapped electrons by Cu^+ are difficult to be transformed to the adsorbed species on the catalyst surface. As a result, Cu^+ may play a negative role as an electron-hole recombination center. Qin *et al.* (2011) demonstrated that it was the heterojunctions between CuO and TiO_2 that contributed to the promotion of the photoactivity. Only one study in the literature (Hirano *et al.*, 1992) indicated that metallic Cu deposited on TiO_2 enhanced the photoefficiency of CO_2 reduction, where Cu metal played the roles as an effective co-catalyst for the reduction of CO_2 and as a reducing species to react with the positive holes simultaneously. On the contrary, Tseng *et al.* (2004) pointed out that the presence of Cu^0 on Cu/TiO_2 obtained by H_2 reduction decreased the production of methanol product from CO_2.

The above controversies in the literature on the effect of Cu valence partially resulted from the uncertainties in the identification of Cu valence because of the typically very small concentration of Cu, the amorphous nature of dispersed Cu, and potential Cu valence change during material handling and characterization. Heat treatment in a reducing atmosphere (e.g., H_2) is usually applied to tailor the Cu valence from as-prepared Cu/TiO_2 samples. However, the Cu valence on a H_2-reduced Cu/TiO_2 samples may have changed when exposed to air environment before XPS analysis or before activity measurement, thus making it difficult and inaccurate to explore which Cu species are most active. Hence, it is very important to use in situ analytical instrumentation and experimental approaches to accurately identify the Cu valence and measure its activity in CO_2 photoreduction. Noticeably, when preparing Cu/TiO_2 in a reducing atmosphere to form Cu^+ or Cu^0 species, defects such as V_O and Ti^{3+} on TiO_2 were most likely created concurrently due to the oxygen loss (Chen *et al.*, 2011; Xiong *et al.*, 2012; Liu *et al.*, 2013a). However, the effect of these defects or the potential synergies between Cu and the defects were often neglected.

In a recent study, Liu *et al.* (2013) engineered Cu/TiO_2 composites with different Cu valences plus V_O/Ti^{3+} sites by heat treatment in H_2 or He, applied in situ XPS and DRIFTS to characterize the Cu valence, and measured their photocatalytic activities immediately after in situ thermal pretreatment. The results demonstrated that the unpretreated, He-pretreated, and H_2-pretreated Cu/TiO_2 surfaces were dominated by Cu^{2+}, Cu^+, and Cu^+/Cu^0, respectively. The mixture of Cu^+/Cu^0 induced by H_2-reduction was more active in charge separation than Cu^+ species alone induced by He-pretreatment. This work also indicated the existence of the synergy between Cu species (particularly Cu^+/Cu^0 mixture) and surface oxygen vacancies on TiO_2, which facilitate the separation of electron-hole pairs and promote electron transfer to adsorbed CO_2.

Carbon materials such as two-dimensional graphene sheets have been used to couple with TiO_2 due to the graphene's unique carrier mobility, high flexible structure, and large surface area. As shown in Fig. 4(d), the deposition of TiO_2 on graphene sheets promotes the electron transfer from TiO_2 to graphene, and extends the light absorption to the visible range. The visible light response of TiO_2/graphene is attributed to the chemical bonding between TiO_2 and the specific sites of carbon that leads to the narrowing of TiO_2 band gap (Zhang *et al.*, 2010). To date, only a few studies have been conducted on TiO_2/graphene for CO_2 photoreduction (Liang *et al.*, 2011; Liang *et al.*, 2012; Tu *et al.*, 2012). The defects in graphene and the contact between graphene and TiO_2 will significantly affect the charge transfer and determine the activity and selectivity of CO_2 conversion. Since the defects in graphene serve as the recombination centers of charge carriers, minimizing the defects in graphene decreased the charge recombination rate (Liang *et al.*, 2011). Moreover, increasing the contact between graphene and TiO_2 favors fast electron transfer from TiO_2 to graphene. The electrons on graphene diffused very quickly due to its larger surface area, which restrained the accumulation of electrons and decreased the local electron density. Consequently, the process of two-electron reduction of CO_2 to CO was facilitated as compared with the process of eight-electron reduction of CO_2 to CH_4 (Tu *et al.*, 2012).

Electron Transfer from Photosensitizer CB to TiO_2 CB

Another approach to enhance visible light activity is to couple TiO_2 with quantum dots (QDs) photosensitizers (e.g., CdSe, PbS, AgBr) that have a narrow band gap and absorb visible light (Wang *et al.*, 2010; Asi *et al.*, 2011; Wang *et al.*, 2011a). Generally, these QDs sensitizers have

a higher conduction band edge than TiO_2. A larger difference between the CBs of QDs and TiO_2 will cause a higher driving force of electron injection from QDs CB to TiO_2 CB. This electron transfer process facilitates the e^-–h^+ separation and improves the visible light activity. If coupling electron trappers (e.g., Pt, Cu) with QDs/TiO_2, the electron transport can be further enhanced in the direction from QDs to TiO_2 and to Pt or Cu. The generation and transfer of charge carriers are closely associated with the dispersion and particles size of the QDs sensitizers. Wang *et al.* (2011) applied PbS QDs to sensitize Cu/TiO_2 for CO_2 photoreduction, and proposed a charge transfer mechanism in PbS/Cu/TiO_2, as shown in Fig. 5(a). Although the CB edge of bulk PbS was slightly lower than that of TiO_2, the CB edge of the smaller PbS particles shifted to a higher energy level due to the quantum confinement, enabling the injection of electrons from 3 or 4 nm PbS to TiO_2. As a result, PbS-(Cu/TiO_2) catalysts showed three times higher activity than Cu/TiO_2 under white-light irradiation.

Electron Transfer between Heterojunctions

A heterojunction, like a diode, is created when two different layers of crystalline semiconductors are placed in conjunction or layered together with alternating or dissimilar band gaps. Both semiconductors in the heterojunctions are photoexcited to generate e^-–h^+ pairs. The energy bias between the two sides will result in the electrons and holes transfer between them. The electrons could transport from the semiconductor with a higher CB to the one with a lower CB. Meanwhile, the holes could transport from the semiconductor with a lower VB to the one with a higher VB. In this respect, the separation and transfer of charge carriers are enhanced, leading to a higher photocatalytic efficiency. Xi *et al.* (2011) developed a nanoporous "French-fires"-shaped TiO_2-ZnO composite, which demonstrated a six times higher activity than P25 for CO_2 photoreduction. Fig. 5(b) shows the charge transfer mechanism in the TiO_2-ZnO heterojunction for CO_2 photoreduction. The photogenerated electrons migrated from ZnO CB to TiO_2 CB, since the CB of ZnO (–0.31 V) was higher than that of TiO_2 (–0.29 V). In the meantime, the holes migrated from TiO_2 VB (2.91 V vs. NHE) to ZnO VB (2.89 V vs. NHE). This literature result demonstrated the significant role of heterjunctions in enhancing photocatalytic performance of TiO_2 by accelerating the charge separation.

Besides ZnO-coupled TiO_2, other semiconductors such as CuO, Cu_2O, and $FeTiO_3$ have been paired with TiO_2 for CO_2 photoreduction (Mor *et al.*, 2008; Roy *et al.*, 2010; Qin *et al.*, 2011; In *et al.*, 2012; Truong *et al.*, 2012). These semiconductors have a narrow band-gap (E_g = 1.8–2.5 eV) and relatively high absorption coefficient in the visible region. Consequently, the heterojunctions formed between these semiconductors and TiO_2 may enhance the separation of charge carriers and the response of visible light simultaneously. It should be noted that in section 3.3.2, we have discussed that CuO and Cu_2O, incorporated on TiO_2, can act as electron trapping sites to enhance electron transfer from TiO_2 to CuO_x. A key factor that determines the function of CuO_x in a CuO_x-TiO_2 composite catalyst system is the concentration and crystal structure of CuO_x. When the

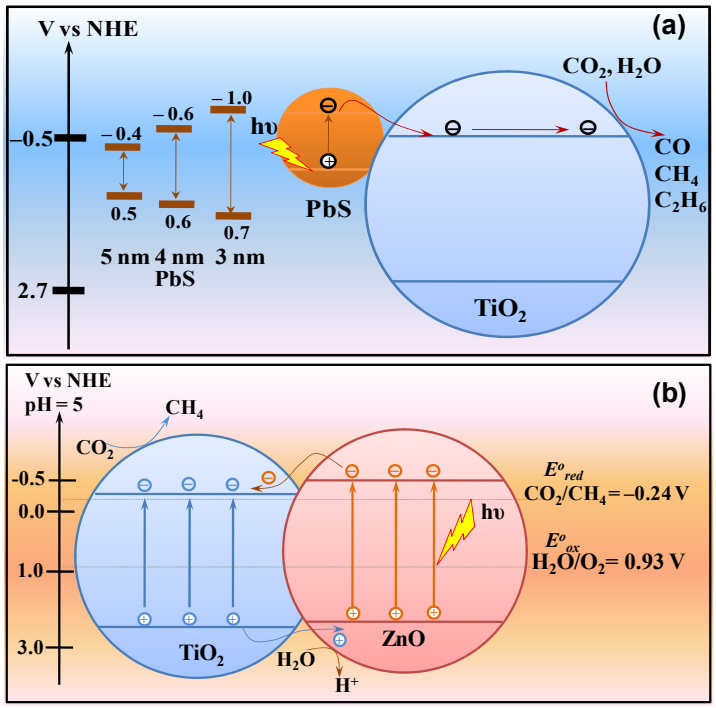

Fig. 5. (a) Band alignment between TiO_2 and PbS QDs with different particles size, and the schematic diagram of the photocatalytic process for CO_2 photoreduction under visible light irradiation. Adapted from (Wang *et al.*, 2011a). (b) Schematic illustration of the band structure and charge separation in the hybrid TiO_2/ZnO composites. Adapted from (Xi *et al.*, 2011).

concentration of CuO_x is small (e.g., 0.1 to 2%), CuO_x is typically amorphous and highly dispersed on the surface of TiO_2. In this case, the dispersed Cu^{2+} or Cu^+ species trap electrons from TiO_2 undergoing redox processes of Cu^{2+}/Cu^+ or Cu^+/Cu^0 (Slamet *et al.*, 2005). When the concentration of CuO_x is very high (close or more than the TiO_2), CuO_x usually exists as crystalline particles and behaves as a semiconductor. In this case, when CuO_x is coupled with TiO_2, the heterojunction effect occurs. Because the TiO_2 CB edge and CuO VB edge are close to each other, photo-excited electrons in the TiO_2 CB could recombine with holes produced in the CuO VB, while higher energy electrons left in the CuO CB reduce CO_2 to hydrocarbons and the holes left in the TiO_2 VB oxide H_2O to O_2 (Roy *et al.*, 2010; Qin *et al.*, 2011; Fan *et al.*, 2013). This charge transfer mechanism at the CuO_x/TiO_2 heterojunction is different from that at the ZnO/TiO_2 heterojunction previous described.

CO_2 PHOTOREDUCTION ON TIO_2-BASED MATERIALS: REACTION PATHWAYS

For the photocatalytic reduction of CO_2 with H_2O over TiO_2-based materials, the reaction pathways generally includes the following steps, i.e., the adsorption of reactants on the catalyst, activation of the adsorbed reactants by the photogenerated charge carriers, formation of surface intermediates, conversion of intermediates to products, desorption of products from catalyst surface, and regeneration of the catalyst. Each of these steps determines the dynamics of the reaction process and affects the final products from CO_2 conversion. In addition, organic Ti-precursors (e.g., titanium isopropoxide), organic solvents (e.g., ethanol), and chloride-containing chemicals (e.g., $CuCl_2$ and H_2PtCl_6) are often used to prepare the photocatalysts. Even after calcination, a certain amount of organic residues (e.g., carbon or hydrocarbons) or inorganic ions (e.g, Cl^-) may still be present on the catalyst surface. These surface contaminants could react with CO_2 and H_2O under photo-irradiation, interfering with the photoinduced reactions and influencing product selectivity. The steps of adsorption/ activation of CO_2 and charge transfer from the catalyst to CO_2 have been discussed in Sections 2 and 3. In this section, the rate limiting step, reaction intermediates, product selectivity, and interferences by the surface contaminants are discussed.

Rate Limiting Step

Only a few studies have been conducted on the investigation of the kinetic models for CO_2 photoreduction, where there are two views about the rate limiting step. The first view is that the activation of CO_2 or H_2O through charge transfer is the rate limiting step. Lin *et al.* (2004) proposed that for CO_2 photoreduction with H_2O, CO_2 reduction and H_2O splitting proceeded competitively at the same Ti-O sites. Uner and Oymak (2012) indicated that the activation of both CO_2 and H_2O through charge transfer is the two important steps in the photocatalytic reduction of CO_2 with H_2O vapor over Pt/TiO_2. The adsorption and accommodation of CO_2 is not limiting the rate of CH_4 formation, while the production of protons and electrons, or the production of hydrogen atoms from H_2O splitting is the rate limiting step in the overall process. Rasko and Solymosi (1994) suggested that the most important step in any reaction of CO_2 is the activation of rather inert and stable CO_2 involving an electron transfer to CO_2.

The second view is that the rate limiting step in CO_2 photoreduction is determined by the dynamics of reactant adsorption and product desorption. Lo *et al.* (2007) found that the photoreduction rate of CO_2 increased linearly with the initial CO_2 concentration. They suggested that CO_2 photoreduction could be a pseudo-first-order reaction, and the adsorption of CO_2 on TiO_2 was the rate limiting step. Slamet *et al.* (2005) reported that the desorption of products was the rate limiting step in the formation of CH_3OH from CO_2 photoreduction over Cu/TiO_2. In addition, Salatin and Alxneit (1997) demonstrated that the reaction rate of CH_4 formation from CO_2 photoreduction increased when the temperature increased from 25 to 200°C. Their kinetic model indicated that at lower temperatures, the desorption of products was the rate limiting step, while at high temperatures, the adsorption of reactants was the rate limiting step. Similarly, in situ DRIFTS analysis in a recent work confirmed that the activities and stabilities of TiO_2 and MgO/TiO_2 were temperature-dependent and associated with the equilibrium of reactants adsorption/intermediates desorption at the catalyst surface (Liu *et al.*, 2013b). The disagreement in the rate limiting step in the literature warrants further studies to advance the understanding of the reaction kinetics of CO_2 photoreduction, involving CO_2 and H_2O adsorption, activation, dissociation and desorption steps at a wider range of temperatures.

Surface Reaction Intermediates

Several studies have been conducted to explore the surface reaction intermediates in the CO_2 photoreduction over bare TiO_2, micro- and meso-porous titanosilicates, and modified TiO_2 (as mentioned in Section 3.3). The photocatalysts, reaction media, reaction intermediates, and products are summarized in Table 1. Table 1 shows that there are a variety of possible reaction intermediates, largely depending on the reaction media. In a solid-gas reaction system involving CO_2 and H_2O vapor, CO_2^-, C•, CO, HCO_3^-, and HCOOH are the primary intermediates. CO_2^- and HCOOH can be converted to CO, while C•, CO and HCO_3^- are considered as the intermediates for the production of hydrocarbons (e.g., CH_4, C_2H_4, C_2H_6). In a solid-liquid reaction system involving dissolved CO_2 in water, CO_2^-, CH_3•, COOH•, and HCHO are the common intermediates, which can be transformed into CH_4, CH_3OH, HCOOH and CH_3CH_2OH.

The type and nature of active sites of the catalyst may also affect the intermediate species and final products. Isolated Ti-sites incorporated into various porous silica materials (e.g., MCM-41, SBA-15, 5A sieves) have been fabricated and applied to CO_2 photoreduction (Lin *et al.*, 2004; Ulagappan and Frei, 2000; Srinivas *et al.*, 2011; Yang *et al.*, 2011; Zhao *et al.*, 2012b). The reaction mechanisms on these supported TiO_2 materials were also investigated. Anpo *et al.* (1995) proposed a mechanism for CO_2

Table 1. The comparison of the reaction intermediates, products and reaction media for CO_2 photoreduction with H_2O on the different photocatalysts from the literature.

Catalysts	Reaction intermediates	Products	Reaction Media	References
TiO_2-anatase	H•, CH_3•, OH•	CH_4, CH_3OH	NaOH solution	(Koci *et al.*, 2009)
TiO_2-brookite	CO_2•, HCOOH	CO, CH_4,	H_2O vapor	(Liu *et al.*, 2012b)
TiO_2-P25	$HCOO^-$, CO_3^{2-}	CH_4	H_2O solution	(Dimitrijevic *et al.*, 2011)
Ti-MCM-41	O^-, OH•	CO	H_2O vapor	(Lin *et al.*, 2004)
Ti-SBA-15	CO, HCOH	CH_4, C_2H_4, C_2H_6	H_2O vapor	(Yang *et al.*, 2011)
$CuTi/SiO_2$	-	CO, CH_4	H_2O vapor	(Li *et al.*, 2010)
CuTi/5A	CO_2•, COOH•, CH_3OH	CH_4, CH_3OH, CH_3COOH, COOH-COOH	Alkaline solution	(Srinivas *et al.*, 2011)
Pt/TiO_2	HCO_3^-	CH_4	H_2O vapor	(Uner and Oymak, 2012)
Au/TiO_2	-	CH_4, C_2H_6, HCHO, CH_3OH	H_2O vapor	(Hou *et al.*, 2011)
Pd/TiO_2	CO_3^{2-}, CO_2(aq), H_2CO_3	CH_4, C_2H_6, C_3H_8	Na_2CO_3 solution	(Dubois and Dubois, 2009)
N-TiO_2	H•, CH_3• HCO_2•, CH_3O_2•, CH_3O_2•,	HCOOH, HCHO, CH_3OH, CH_4	$KHCO_3$ solution	(Peng *et al.*, 2012)
$FeTiO_3/TiO_2$	H_2CO_3, HCO_2•, HCOOH	CH_3OH	$NaHCO_3$ solution	(Truong *et al.*, 2012)
CuO/TiO_2	C residue	CH_4	H_2O vapor	(Yang *et al.*, 2010)
CuO-TiO_2	HCOOH, HCHO	$HCOOCH_3$	CH_3OH solution	(Qin *et al.*, 2011)
CuO_x/TiO_2	CO_2•, HCO_3^-	CO, CH_4	H_2O vapor	(Liu *et al.*, 2012a)
$AgBr/TiO_2$	CO_2•, C•, CH_3•	CH_4, CH_3OH, CO, CH_3CH_2OH	$KHCO_3$ solution	(Asi *et al.*, 2011)
Pt-Cu/TiO_2	CO, OH•	CO, H_2, CH_4, olefin, branched paraffin, alkanes	H_2O vapor	(Varghese *et al.*, 2009)
$Ag/ALa_4Ti_4O_{17}$ (A: Ca, Sr, Ba)	-	CO, HCOOH, H_2, O_2	H_2O vapor	(Iizuka *et al.*, 2011)
Cu-I/TiO_2	H•, CO•, C•	CO, CH_4, CH_3Cl	H_2O vapor	(Zhang *et al.*, 2012)
Ni-N/TiO_2	-	CH_3OH	NaOH, Na_2SO_3 solution	(Fan *et al.*, 2011)
M-N/TiO_2 (M: Pt, Au, Ag)	C residues	CH_4	H_2O vapor	(Li *et al.*, 2012)

photoreduction with H_2O on TiO_2 anchored within a zeolite catalyst (Scheme 1). CO_2 and H_2O molecules interact with the photoexcited Ti^{3+}–O^-* sites, inducing the formation of H atoms, OH radicals, and carbon species. These intermediate radicals combine with each other to form CH_4 and CH_3OH. In addition, the reduction of CO_2 and the decomposition of H_2O proceed competitively on the same Ti^{3+}–O^-* sites, depending on the ratio of H_2O to CO_2. In Yang's work (Yang *et al.*, 2011), three hydrocarbons (i.e., CH_4, C_2H_4, and C_2H_6) were produced from photocatalytic reduction of CO_2 with H_2O over Ti-SBA-15. For the formation mechanism of the hydrocarbons, Ti-OH serves as the active site for the adsorption of CO_2 and H_2O, where CO and hydroperoxo (Ti–OOH) intermediates are generated and subsequently converted to HCHO. One HCHO was converted to CH_4 by reaction with photo-activated H_2O; two HCHO combined with each other to yield C_2H_4, and the reaction of two HCHO with one H_2O led to the formation of C_2H_6.

The intermediates and reaction pathways for CO_2 photoreduction were related to the crystal phase and defects in TiO_2 as well. In situ DRIFTS studies have been done to explore the surface intermediates and reaction mechanism of CO_2 photoreduction on defective and defect-free TiO_2 (Liu *et al.*, 2012b). In the dark, upon the exposure of catalysts to CO_2 and H_2O, the adsorbed species on the surfaces of defect-free TiO_2 anatase and brookite were similar, including mainly H_2O, bicarbonates, and carbonates species. Subsequently under photo-illumination, no CO_2^- or other new species were formed on defect-free TiO_2, and the adsorbed H_2O was stable. By contrast, CO_2^- was favourably formed on the defective TiO_2 anatase. Fig. 6 shows the IR spectra of CO_2 and H_2O interaction with the defective anatase in the dark and under the photoillumination. At 5 min, the early stage of adsorption, CO_2^- species (1670 and 1247 cm^{-1}) were formed even in the dark (Fig. 6(a)). Although it disappeared by prolonging the adsorption time to 15 min, subsequent photo-illumination induced the reappearance of CO_2^-, the intensity of which increased with the irradiation time (Fig. 6(b)). The re-presence of CO_2^- is an evidence that the photoexcited electrons that were trapped in the defect sites transferred to the adsorbed CO_2 on the defective surface. In the case of brookite, CO_2^- was formed on the defective brookite in the dark but was not represent unde photoillumination in the presence of H_2O. This is likely due to the faster reaction of CO_2^- with H^+ (generated from H_2O) on brookite.

Table 2 shows the tentative mechanism for CO and CH_4 formation on the defective anatase and brookite (Liu *et al.*, 2012b). CO_2^- and HCO_3^- were formed on both the defective anatase and brookite (Reactions 2 and 3). CO_2^- could be reduced to CO via reaction with H^+ (Reaction 4), self-transformation (Reaction 5), or direct dissociation by healing the V_O sites (Reaction 6). A unique intermediate, HCOOH, was only formed on the defective brookite (Reactions 8 and

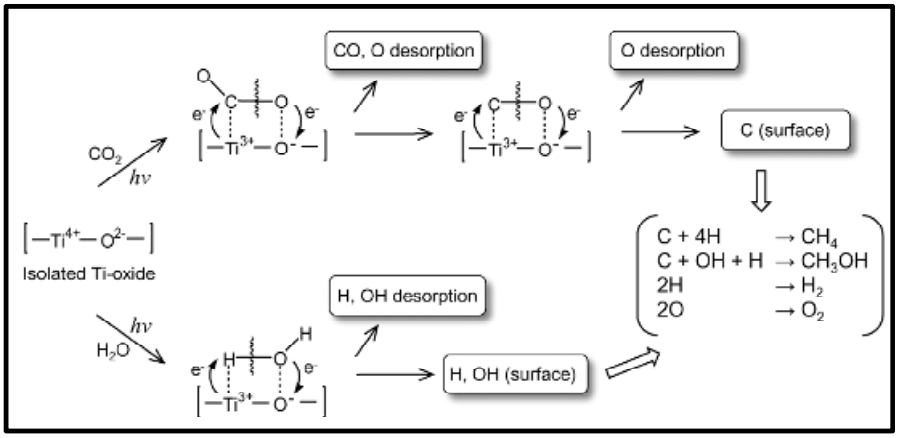

Scheme 1. Schematic representation of the photocatalytic reduction of CO_2 with H_2O on the anchored titanium oxide. Reproduced with permission from (Anpo *et al.*, 1995).

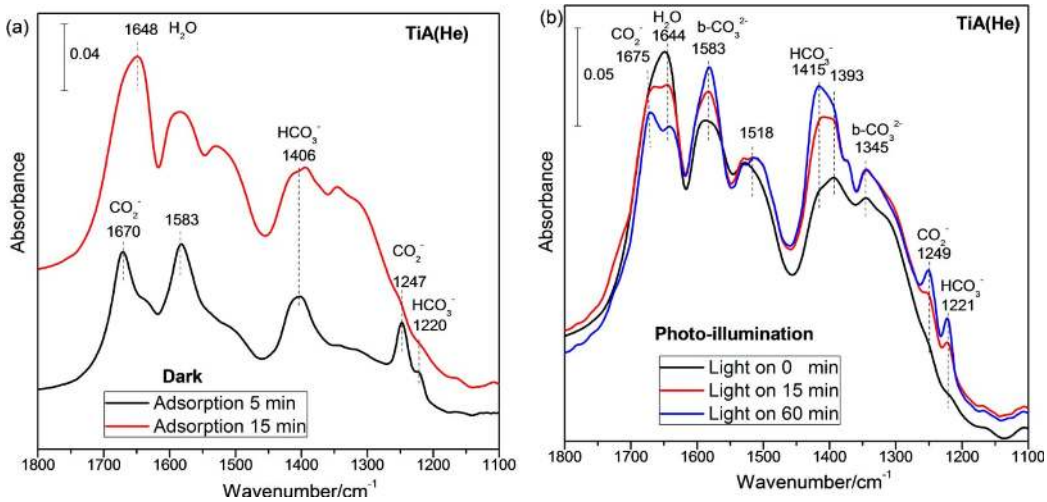

Fig. 6. In situ DRIFTS spectra of CO_2 and H_2O interaction with defective anatase (i.e., TiA(He)) (a) in the dark, and (b) subsequently irradiated by UV-visible light as a function of time. Reproduced with permission from (Liu *et al.*, 2012b).

Table 2. The possible reaction pathways for the formation of CO and CH_4 from CO_2 photoreduction with H_2O vapor on oxygen-deficient TiO_2 anatase and brookite phases. Reproduced with permission from (Liu *et al.*, 2012b).

Phase	CO_2 photoreduction with H_2O vapor			
Defective TiO_2 anatase and brookite	$H_2O + h^+ \rightarrow H^+ + OH\bullet$	(1)	$CO_2 + Ti^{3+} \rightarrow Ti^{4+}–CO_2^-$	(2)
	$OH\bullet + CO_2^- \rightarrow HCO_3^-$	(3)	$CO_2^- + H^+ + e^- \rightarrow CO + OH^-$	(4)
	$CO_2^- + CO_2^- \rightarrow CO + CO_3^{2-}$	(5)	$CO_2^- + [Ti^{3+}–V_O–Ti^{4+}] \rightarrow CO + [Ti^{4+}–O^{2-}–Ti^{4+}]$	(6)
	$CO, HCO_3^-, HCOOH \xrightarrow{e^-} C_{(ads)}\bullet \xrightarrow{H\bullet} CH_3\bullet \xrightarrow{H\bullet} CH_4$			(7)
Defective TiO_2 brookite	$CO_2 + 2H^+ + 2e^- \rightarrow HCOOH$	(8)	$CO_2^- + 2H^+ + e^- \rightarrow HCOOH$	(9)
	$HCOOH \rightarrow CO + H_2O$	(10)	$CO, HCOOH \xrightarrow{e^-, H^+} CH_4$	(11)

9) and could be dissociated to CO subsequently (Reaction 10). Table 2 shows that CO_2 photoreduction to CO probably undergoes different mechanisms on defective anatase and brookite through different surface intermediates (e.g., CO_2^- on anatase; CO_2^- and HCOOH on brookite). For CH_4 formation, possible intermediates are CO, HCO_3^-, and HCOOH, which may be converted to CH_4 via a multi-electron transfer process, once dissociated hydrogen atoms are available (Reactions 7 and 11).

Product Selectivity

Table 1 clearly demonstrates the variety of possible products from CO_2 photoreduction, such as H_2, O_2, CO, CH_4, CH_4OH, HCOOH, HCHO and other hydrocarbons, indicating the lack of control of product selectivity in CO_2 conversion over TiO_2-based photocatalysts. Table 1 also shows that the product selectivity is dependent on the types of reaction media and catalyst composition. In the gas phase reaction environment, CO and CH_4 are reported as

the major C1 chemicals; while in the aqueous environment, alcohols (e.g., CH_3OH, CH_3CH_2OH) are mainly produced. In addition, the incorporation of metals or metal oxides to TiO_2 facilitated the production of hydrocarbons such as CH_4 and CH_3OH.

As shown in Table 1, CO, CH_4, and CH_3OH are the three most common products from CO_2 photoreduction. Scheme 2 illustrates the possible reaction pathways to form those three products. CO can be formed via the intermediates of CO_2^- and HCOOH, respectively. The CO_2^- anions can be converted to CO via the reaction with H• radical, self-transformation, or dissociation on the oxygen vacancy sites (Scheme 2(a)). Another route for CO formation is the photodecomposition of HCOOH (Scheme 2(b)). The generated CO can serve as the intermediate for the subsequent formation of CH_4 and CH_3OH through deoxygenation (Scheme 2(c)). In this process, the oxidation states of carbon decrease from +IV (CO_2), to +II (CO), to 0 (C), to –I (CH•), and then to –III (CH_3•). The CH_3• can either combine with OH• radical to form CH_3OH or with H• radical to form CH_4. Another pathway for CH_3OH and CH_4 formation is the hydrogenation of CO_2 with H atoms through the HCOOH intermediate (Scheme 2d). In this route, the oxidation states of carbon change from +IV (CO_2), to +II (HCOOH), to 0 (HCHO), to –II (CH_3OH), and then to –IV (CH_4). Dhakshinamoorthy *et al.* (2012) suggested that the two reaction routes (Scheme 2(c) or 2(d)) depend on whether the CO_2 hydrogenation step is faster or slower than the CO_2 deoxygenation step. If CO_2 hydrogenation is faster than deoxygenation, Scheme 2(d) will proceed. Otherwise, Scheme 2(c) will proceed.

Nevertheless, it is difficult to selectively control the occurrence of the reaction routes proposed in Scheme 2. One factor that significantly influences the product selectivity is the catalyst composition/properties. Wu and Huang (2010) found that the addition of Cu species enhanced the formation of CH_3OH on Cu/TiO_2 due to the migration of H atoms on the Cu sites via the reduction of H^+ with trapped electrons. The H-Cu sites promote the hydrogenation of the intermediates to generate CH_3OH. Anpo *et al.* (1997) reported a unique role of Pt metal on Ti/Y-zeolites for CO_2 photoreduction, besides the conventional role of Pt in promoting charge transfer. They found that carbon radials and H atoms were generated on the same Pt metal sites, and thus CH_4 formation was facilitated by Pt. Because the OH• radicals were formed at different sites from where the carbon radicals were formed, the presence of Pt metal suppressed the formation of CH_3OH.

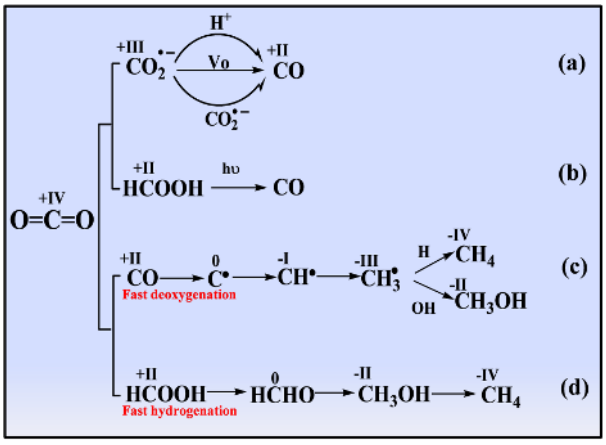

Scheme 2. Proposal of reaction pathways for the formation of CO, CH_4 and CH_3OH in the photocatalytic CO_2 reduction. Adapted from (Dhakshinamoorthy *et al.*, 2012; Liu *et al.*, 2012b).

Interference of Surface Contaminants

Recently, Yang *et al.* (2010) raised a concern on the interference of surface contaminants on the catalyst such as carbon residues that may participate in the CO_2 photoreduction and affect the activity and selectivity. The surface contaminants are possibly originated from the Ti-precursors and the solvents during the catalyst synthesis process. As suggested by Yang *et al.* (2010), the carbon residues were derived from the use of Ti-alkoxides and organic solvents. Calcination in air environment could not completely remove these carbon residues, while exposure of the catalyst to H_2O vapor and UV-irradiation was effective to clean the catalyst surface. Through the DRIFTS analysis using ^{13}C labelled CO_2, Yang *et al.* (2010) demonstrated that carbon residues can react with CO_2 and H_2O to form CO over Cu-promoted TiO_2, i.e., $^{13}CO_2 + {}^{12}C \rightarrow {}^{13}CO + {}^{12}CO$ and $H_2O + {}^{12}C \rightarrow {}^{12}CO + H_2$.

Other surface contaminants like chlorine species may interfere with the CO_2 photoreduction. A recent work reported that an undesirable product (i.e., CH_3Cl) was formed during CO_2 photoreduction on copper and iodine co-modified TiO_2 when a chlorinated Cu-precursor was used (Zhang *et al.*, 2012). The path to CH_3Cl formation is likely through the reaction of a methyl radical (CH_3•) and a chlorine radical (Cl•), the latter of which is generated by Cl ions reacting with photoexcited holes. The generation of CH_3Cl indirectly confirms that methyl radicals, likely derived from surface adsorbed carbon species, is a reaction intermediate for CO_2 photoreduction. The above studies on the effect of surface contaminants can provide two insights in the field of CO_2 photoreduction. First, it is important for the researchers to choose the right chemical precursors or methods to prepare catalysts to avoid or remove surface contaminants and to ensure the accuracy of their results. Second, if properly applied, intentionally contaminated surfaces can be useful to help explore and decouple the complex reaction mechanism.

CONCLUSIONS AND FUTURE PROSPECTS

In this review we have summarized the literature results on the mechanism of CO_2 photoreduction with H_2O using TiO_2-based photocatalysts, including CO_2 adsorption/dissociation, charge transfer mechanism, and reaction pathways/product selectivity. Three primary factors, TiO_2 crystal phase, surface defects, and material modifications, are reviewed. The literature has demonstrated that (1) CO_2 activation and dissociation process can be promoted by creating defect disorders on TiO_2 surface (e.g., Ti^{3+} and oxygen vacancy), (2) the charge separation and transfer

can be enhanced by tailoring the crystal phase of TiO_2 (e.g., mixture of anatase/brookite or anatase/rutile), engineering the defects in TiO_2, and incorporating modifiers with TiO_2 (e.g., metals, metal oxides, graphene, quantum dot sensitizers), and (3) the crystal phase, active sites, modifiers, and reaction media all affect the types of surface reaction intermediates and final products. One has to be aware that several challenges still exist in this filed. First, there is a great need to promote the CO_2 conversion efficiency by orders of magnitude, since the current efficiency is very low and far from practical applications. Second, there is lack of detailed experimental evidences for the charge transfer directions and dynamics. Third, the surface intermediates, reaction pathways, and reaction kinetics for CO_2 photoredeuction have not been clearly understood. It is also difficult to control or even rationalize the product selectivity.

In light of this review, we suggest that future research can be conducted in the following directions to extend the understanding in the CO_2 photoreduction mechanism and to design more efficient photocatalysts: (1) Taking the advantages of the combined effects of mixed crystal phase, defect-disorders, and material modifications to rationally design an efficient, selective, long-term stable, and regenerable TiO_2-based photocatalysts; (2) Studying the direction of electron transfer in TiO_2-based materials by EPR or in situ EPR (particularly the interfacial electron transfer between two phases or between TiO_2 and modifiers), and correlate it with materials properties and photocatalytic activities; (3) Applying in situ FTIR to monitor the surface reaction intermediates and to investigate the strategies to control product selectivity; (4) Investigating the rate limiting step and the dynamics of the reactant adsorption/product desorption process by conducting photocatalytic reactions at different temperatures.

ACKNOWLEDGEMENTS

The authors acknowledge the support from National Science Foundation (NSF CBET-1067233).

REFERENCES

An, C., Wang, J., Jiang, W., Zhang, M., Ming, X., Wang, S. and Zhang, Q. (2012). Strongly visible-light Responsive Plasmonic Shaped AgX:Ag (X = Cl, Br) Nanoparticles for Reduction of CO_2 to Methanol. *Nanoscale* 4: 5646–5650.

Anpo, M., Yamashita, H., Ichihashi, Y. and Ehara, S. (1995). Photocatalytic Reduction of CO_2 with H_2O on Various Titanium-Oxide Catalysts. *J. Electroanal. Chem.* 396: 21–26.

Anpo, M., Yamashita, H., Ichihashi, Y., Fujii, Y. and Honda, M. (1997). Photocatalytic Reduction of CO_2 with H_2O on Titanium Oxides Anchored within Micropores of Zeolites: Effects of the Structure of the Active Sites and the Addition of Pt. *J. Phys. Chem. B* 101: 2632–2636.

Asahi, R., Morikawa, T., Ohwaki, T., Aoki, A. and Taga (2001). Visible-Light Photocatalysis in Nitrogen-Doped Titanium Oxides. *Science* 293: 269–271.

Aschauer, U., He, Y.B., Cheng, H.Z., Li, S.C., Diebold, U. and Selloni, A. (2010). Influence of Subsurface Defects on the Surface Reactivity of TiO_2: Water on Anatase (101). *J. Phys. Chem. C* 114: 1278–1284.

Ashley, M., Magiera, C., Ramidi, P., Blackburn, G., Scott, T.G., Gupta, R., Wilson, K., Ghosh, A. and Biswas, A. (2012). Nanomaterials and Processes for Carbon Capture and Conversion into Useful by-products for a Sustainable Energy Future. *Greenhouse Gases Sci. Technol.* 2: 419–444.

Asi, M.A., He, C., Su, M., Xia, D., Lin, L., Deng, H., Xiong, Y., Qiu, R. and Li, X.Z. (2011). Photocatalytic Reduction of CO_2 to Hydrocarbons Using AgBr/TiO_2. *Catal. Today* 175: 256–263.

Bickley, R.I., Gonzalezcarreno, T., Lees, J.S., Palmisano, L. and Tilley, R.J.D. (1991). A Structural Investigation of Titanium-Dioxide Photocatalysts. *J. Solid State Chem.* 92: 178−190.

Boppella, R., Basak, P. and Manorama, S. V. (2012). Viable Method for the Synthesis of Biphasic TiO_2 Nanocrystals with Tunable Phase Composition and Enabled Visible-light Photocatalytic Performance. *ACS Appl. Mater. Interfaces* 4: 1239−1246.

Chen, X.B. and Burda, C. (2008). The Electronic Origin of the Visible-Light Absorption Properties of C-, N- and S-Doped TiO_2 Nanomaterials. *J. Am. Chem. Soc.* 130: 5018–5019.

Chen, X.B., Liu, L., Yu, P.Y. and Mao, S.S. (2011). Increasing Solar Absorption for Photocatalysis with Black Hydrogenated Titanium Dioxide Nanocrystals. *Science* 331: 746–750.

Chiarello, G.L., Di Paola, A., Palmisano, L. and Selli, E. (2011). Effect of Titanium Dioxide Crystalline Structure on the Photocatalytic Production of Hydrogen. *Photochem. Photobiol. Sci.* 10: 355–360.

DeSario, P.A., Chen, L., Graham, M.E. and Gray, K.A. (2011). Effect of Oxygen Deficiency on the Photoresponse and Reactivity of Mixed Phase Titania Thin Films. *J. Vac. Sci. Technol., A* 29: 031508.

Dhakshinamoorthy, A., Navalon, S., Corma, A. and Garcia, H. (2012). Photocatalytic CO_2 Reduction by TiO_2 and Related Titanium Containing Solids. *Energy Environ. Sci.* 5: 9217–9233.

Dimitrijevic, N.M., Vijayan, B.K., Poluektov, O.G., Rajh, T., Gray, K.A., He, H.Y. and Zapol, P. (2011). Role of Water and Carbonates in Photocatalytic Transformation of CO_2 to CH_4 on Titania. *J. Am. Chem. Soc.* 133: 3964–3971.

Dubois, M.R. and Dubois, D.L. (2009). Development of Molecular Electrocatalysts for CO_2 Reduction and H_2 Production/Oxidation. *Acc. Chem. Res.* 42: 1974–1982.

Fan, J., Liu, E.Z., Tian, L., Hu, X.Y., He, Q. and Sun, T. (2011). Synergistic Effect of N and Ni^{2+} on Nanotitania in Photocatalytic Reduction of CO_2. *J. Environ. Eng.* 137: 171–176.

Fan, W., Zhang, Q. and Wang, Y. (2013). Semiconductor-based Nanocomposites for Photocatalytic H_2 Production and CO_2 Conversion. *Phys. Chem. Chem. Phys.* 15: 2632−2649.

Furler, P., Scheffe, J.R. and Steinfeld, A. (2012). Syngas

Production by Simultaneous Splitting of H_2O and CO_2 via Ceria Redox. *Energy Environ. Sci.* 5: 6098–6103.

Gai, L.G., Duan, X.Q., Jiang, H.H., Mei, Q.H., Zhou, G.W., Tian, Y. and Liu, H. (2012). One-pot Synthesis of Nitrogen-doped TiO_2 Nanorods with Anatase/Brookite Structures and Enhanced Photocatalytic Activity. *CrystEngComm* 14: 7662–7671.

He, H., Liu, C., Dubois, K.D., Jin, T., Louis, M.E. and Li, G. (2012). Enhanced Charge Separation in Nanostructured TiO_2 Materials for Photocatalytic and Photovoltaic Applications. *Ind. Eng. Chem. Res.* 51: 11841−11849.

He, H.Y., Zapol, P. and Curtiss, L.A. (2010). A Theoretical Study of CO_2 Anions on Anatase (101) Surface. *J. Phys. Chem. C* 114: 21474–21481.

Hirano, K., Inoue, K. and Yatsu, T. (1992). Photocatalysed Reduction of CO_2 in Aqueous TiO_2 Suspension Mixed with Copper Powder. *J. Photochem. Photobiol., A* 64: 255–258.

Hoang, S., Berglund, S.P., Hahn, N.T., Bard, A.J. and Buddie Mullins, C. (2012). Enhancing Visible Light Photo-oxidation of Water with TiO_2 Nanowire Arrays via Cotreatment with H_2 and NH_3: Synergistic Effects between Ti^{3+} and N. *J. Am. Chem. Soc.* 134: 3659–3662.

Hou, W., Hung, W.H., Pavaskar, P., Goeppert, A., Aykol, M. and Cronin, S.B. (2011). Photocatalytic Conversion of CO_2 to Hydrocarbon Fuels via Plasmon-Enhanced Absorption and Metallic Interband Transitions. *ACS Catal.* 1: 929–936.

Hurum, D.C., Agrios, A.G., Gray, K.A., Rajh, T. and Thurnauer, M.C. (2003). Explaining the Enhanced Photocatalytic Activity of Degussa P25 Mixed-Phase TiO_2 Using EPR. *J. Phys. Chem. B* 107: 4545–4549.

Ihara, T., Miyoshi, M., Iriyama, Y., Matsumoto, O. and Sugihara, S. (2004). Visible-light-active Titanium Oxide Photocatalyst Realized by an Oxygen-deficient Structure and by Nitrogen Doping *Appl. Catal., B* 42: 403–409.

Iizuka, K., Wato, T., Miseki, Y., Saito, K. and Kudo, A. (2011). Photocatalytic Reduction of Carbon Dioxide over Ag Cocatalyst-Loaded $ALa_4Ti_4O_{15}$ (A = Ca, Sr, and Ba) Using Water as a Reducing Reagent. *J. Am. Chem. Soc.* 133: 20863–20868.

In, S.I., Vaughn, D.D., II and Schaak, R.E. (2012). Hybrid $CuO\text{-}TiO_{2-x}N_x$ Hollow Nanocubes for Photocatalytic Conversion of CO_2 into Methane under Solar Irradiation. *Angew. Chem. Int. Ed.* 51: 3915–3918.

Indrakanti, V.P., Kubicki, J.D. and Schobert, H.H. (2009). Photoinduced Activation of CO_2 on Ti-based Heterogeneous Catalysts: Current State, Chemical Physics-based Insights and Outlook. *Energy Environ. Sci.* 2: 745–758.

Indrakanti, V.P., Kubicki, J.D. and Schobert, H.H. (2011). Photoinduced Activation of CO_2 on TiO_2 Surfaces: Quantum Chemical Modeling of CO_2 Adsorption on Oxygen Vacancies. *Fuel Process. Technol.* 92: 805–811.

Irie, H., Kamiya, K., Shibanuma, T., Miura, S., Tryk, D. A., Yokoyama, T. and Hashimoto, K. (2009). Visible Light-Sensitive Cu(II)-Grafted TiO_2 Photocatalysts: Activities and X-ray Absorption Fine Structure Analyses. *J. Phys. Chem. C* 113: 10761–10766.

Jiao, W., Wang, L., Liu, G., Lu, G.Q. and Cheng, H.M. (2012a). Hollow Anatase TiO_2 Single Crystals and Mesocrystals with Dominant {101} Facets for Improved Photocatalysis Activity and Tuned Reaction Preference. *ACS Catal.* 2: 1854–1859.

Jiao, Y., Chen, F., Zhao, B., Yang, H. and Zhang, J. (2012b). Anatase Grain Loaded Brookite Nanoflower Hybrid with Superior Photocatalytic Activity for Organic Degradation. *Colloids Surf., A* 402: 66–71.

Justicia, I., Ordejon, P., Canto, G., Mozos, J.L., Fraxedas, J., Battiston, G.A., Gerbasi, R. and Figueras, A. (2002). Designed Self-Doped Titanium Oxide Thin Films for Efficient Visible-Light Photocatalysis. *Adv. Mater.* 14: 1399–1402.

Kawahara, T., Konishi, Y., Tada, H., Tohge, N., Nishii, J. and Ito, S. (2002). A Patterned TiO_2(anatase)/TiO_2(rutile) Bilayer-type Photocatalyst: Effect of the Anatase/Rutile Junction on the Photocatalytic Activity. *Angew. Chem. Int. Ed.* 41: 2811–2813.

Koci, K., Obalova, L., Matejova, L., Placha, D., Lacny, Z., Jirkovsky, J. and Solcova, O. (2009). Effect of TiO_2 Particle Size on the Photocatalytic Reduction of CO_2. *Appl. Catal., B* 89: 494–502.

Koci, K., Mateju, K., Obalova, L., Krejcikova, S., Lacny, Z., Placha, D., Capek, L., Hospodkova, A. and Solcova, O. (2010). Effect of Silver Doping on the TiO_2 for Photocatalytic Reduction of CO_2. *Appl. Catal., B* 96: 239–244.

Kubacka, A., Fernandez-Garcia, M. and Colon, G. (2012). Advanced Nanoarchitectures for Solar Photocatalytic Applications. *Chem. Rev.* 112: 1555–1614.

Lee, J., Sorescu, D.C. and Deng, X.Y. (2011). Electron-Induced Dissociation of CO_2 on TiO_2(110). *J. Am. Chem. Soc.* 133: 10066–10069.

Li, G.H. and Gray, K.A. (2007). The Solid-solid Interface: Explaining the High and Unique Photocatalytic Reactivity of TiO_2-based Nanocomposite Materials. *Chem. Phys.* 339: 173–187.

Li, G.H., Dimitrijevic, N.M., Chen, L., Rajh, T. and Gray, K.A. (2008a). Role of Surface/Interfacial Cu^{2+} Sites in the Photocatalytic Activity of Coupled $CuO\text{-}TiO_2$ Nanocomposites. *J. Phys. Chem. C* 112: 19040–19044.

Li, G.H., Ciston, S., Saponjic, Z.V., Chen, L., Dimitrijevic, N.M., Rajh, T. and Gray, K.A. (2008b). Synthesizing Mixed-phase TiO_2 Nanocomposites Using a Hydrothermal Method for Photo-oxidation and Photoreduction Applications. *J. Catal.* 253: 105–110.

Li, X.K., Zhuang, Z.J., Li, W. and Pan, H.Q. (2012). Photocatalytic Reduction of CO_2 over Noble Metal-loaded and Nitrogen-doped Mesoporous TiO_2. *Appl. Catal., A* 429: 31–38.

Li, Y., Wang, W.N., Zhan, Z.L., Woo, M.H., Wu, C.Y. and Biswas, P. (2010). Photocatalytic Reduction of CO_2 with H_2O on Mesoporous Silica Supported Cu/TiO_2 Catalysts. *Appl. Catal., B* 100: 386–392.

Liang, Y.T., Vijayan, B.K., Gray, K.A. and Hersam, M.C. (2011). Minimizing Graphene Defects Enhances Titania Nanocomposite-Based Photocatalytic Reduction of CO_2 for Improved Solar Fuel Production. *Nano Lett.* 11: 2865–

2870.

Liang, Y.T., Vijayan, B.K., Lyandres, O., Gray, K.A. and Hersam, M.C. (2012). Effect of Dimensionality on the Photocatalytic Behavior of Carbon-Titania Nanosheet Composites: Charge Transfer at Nanomaterial Interfaces. *J. Phys. Chem. Lett.* 3: 1760–1765.

Lin, W.Y., Han, H.X. and Frei, H. (2004). CO_2 Splitting by H_2O to CO and O_2 under UV Light in TiMCM-41 Silicate Sieve. *J. Phys. Chem. B* 108:18269–18273.

Lin, Z.S., Orlov, A., Lambert, R.M. and Payne, M.C. (2005). New Insights into the Origin of Visible Light Photocatalytic Activity of Nitrogen-doped and oxygen-deficient Anatase TiO_2. *J. Phys. Chem. B* 109: 20948–20952.

Liu, L.J., Zhao, C.Y. and Li, Y. (2012a). Spontaneous Dissociation of CO_2 to CO on Defective Surface of Cu(I)/TiO_{2-x} Nanoparticles at Room Temperature. *J. Phys. Chem. C* 116: 7904–7912.

Liu, L.J., Zhao, H.L., Andino, J.M. and Li, Y. (2012b). Photocatalytic CO_2 Reduction with H_2O on TiO_2 Nanocrystals: Comparison of Anatase, Rutile, and Brookite Polymorphs and Exploration of Surface Chemistry. *ACS Catal.* 2: 1817–1828.

Liu, L.J., Gao, F., Zhao, H.L. and Li, Y. (2013a). Tailoring Cu Valence and Oxygen Vacancy in Cu/TiO_2 Catalysts for Enhanced CO_2 Photoreduction Efficiency. *Appl. Catal., B* 134–135: 49–358.

Liu, L.J., Zhao, C.Y., Zhao, H.L., Pitts, D. and Li, Y. (2013b). Porous Microspheres of MgO-patched TiO_2 for CO_2 Photoreduction with H_2O Vapor: Temperature-dependent Activity and Stability. *Chem. Commun.* 49: 3664–3666.

Lo, C.C., Hung, C.H., Yuan, C.S. and Wu, J.F. (2007). Photoreduction of Carbon Dioxide with H_2 and H_2O over TiO_2 and ZrO_2 in a Circulated Photocatalytic Reactor. *Sol. Energy Mater. Sol. Cells* 91: 1765–1774.

Markovits, A., Fahmi, A. and Minot, C. (1996). A Theoretical Study of CO_2 Adsorption on TiO_2. *THEOCHEM* 371: 219–235.

Mor, G.K., Varghese, O.K., Wilke, R.H.T., Sharma, S., Shankar, K., Latempa, T.J., Choi, K.S. and Grimes, C.A. (2008). p-type Cu-Ti-O Nanotube Arrays and Their Use in Self-biased Heterojunction Photoelectrochemical Diodes for Hydrogen Generation. *Nano Lett.* 8: 1906–1911.

Mori, K., Yamashita, H. and Anpo, M. (2012). Photocatalytic Reduction of CO_2 with H_2O on Various Titanium Oxide Photocatalysts. *RSC Adv.* 2: 3165–3172.

Noda, H., Oikawa, K., Ogata, T., Matsuki, K. and Kamata, H. (1986). Preparation of Titanium(IV) Oxides and Its Characterization. *Chem. Soc. Jpn.* 8: 1084–1090.

Nowotny, J., Bak, T., Nowotny, M.K. and Sheppard, L.R. (2006). TiO_2 Surface Active Sites for Water Splitting. *J. Phys. Chem. B* 110: 18492–18495.

Nowotny, M.K., Sheppard, L.R., Bak, T. and Nowotny, J. (2008). Defect Chemistry of Titanium Dioxide. Application of Defect Engineering in Processing of TiO_2-based Photocatalysts. *J. Phys. Chem. C* 112: 5275–5300.

Pan, H., Gu, B.H. and Zhang, Z.Y. (2009). Phase-Dependent Photocatalytic Ability of TiO_2: A First-Principles Study. *J. Chem. Theory Comput.* 5: 3074–3078.

Panayotov, D.A., Burrows, S.P. and Morris, J.R. (2012). Infrared Spectroscopic Studies of Conduction Band and Trapped Electrons in UV-Photoexcited, H-Atom n-Doped, and Thermally Reduced TiO_2. *J. Phys. Chem. C* 116: 4535–4544.

Peng, Y.P., Yeh, Y.T., Shah, S.I. and Huang, C.P. (2012). Concurrent Photoelectrochemical Reduction of CO_2 and Oxidation of Methyl Using Nitrogen-doped TiO_2. *Appl. Catal., B* 123–124: 414–423.

Pipornpong, W., Wanbayor, R. and Ruangpornvisuti, V. (2011). Adsorption CO_2 on the Perfect and Oxygen Vacancy Defect Surfaces of Anatase TiO_2 and its Photocatalytic Mechanism of Conversion to CO. *Appl. Surf. Sci.* 257: 10322–10328.

Qin, S.Y., Xin, F., Liu, Y.D., Yin, X.H. and Ma, W. (2011). Photocatalytic Reduction of CO_2 in Methanol to Methyl Formate over CuO-TiO_2 Composite Catalysts. *J. Colloid Interface Sci.* 356: 257–261.

Rasko, J. and Solymosi, F. (1994). Infrared Spectroscopic Study of the Photoinduced Activation of CO_2 on TiO_2 and Rh/TiO_2 Catalysts. *J. Phys. Chem.* 98: 7147–7152.

Rodriguez, M.M., Peng, X.H., Liu, L.J., Li, Y. and Andino, J.M. (2012). A Density Functional Theory and Experimental Study of CO_2 Interaction with Brookite TiO_2. *J. Phys. Chem. C* 116: 19755–19764.

Roy, S.C., Varghese, O.K., Paulose, M. and Grimes, C.A. (2010). Toward Solar Fuels: Photocatalytic Conversion of Carbon Dioxide to Hydrocarbons. *ACS Nano* 4: 1259–1278.

Saladin, F. and Alxneit, I. (1997). Temperature Dependence of the Photochemical Reduction of CO_2 in the Presence of H_2O at the Solid/Gas Interface of TiO_2. *J. Chem. Soc., Faraday Trans.* 93: 4159–4165.

Sasirekha, N., Basha, S.J.S. and Shanthi, K. (2006). Photocatalytic Performance of Ru Doped Anatase Mounted on Silica for Reduction of Carbon Dioxide. *Appl. Catal., B* 62: 169–180.

Schilke, T.C., Fisher, I.A. and Bell, A.T. (1999). In Situ Infrared Study of Methanol Synthesis from CO_2/H_2O on Titania and Zirconia Promoted Cu/SiO_2. *J. Catal.* 184: 144–156.

Schobert, H.H., Indrakanti, V.P. and Kubicki, J.D. (2008). Quantum Chemical Modeling of Ground States of CO_2 Chemisorbed on Anatase (001), (101), and (010) TiO_2 Surfaces. *Energy Fuels* 22: 2611–2618.

Shkrob, I.A., Marin, T.W., He, H.Y. and Zapol, P. (2012). Photoredox Reactions and the Catalytic Cycle for Carbon Dioxide Fixation and Methanogenesis on Metal Oxides. *J. Phys. Chem. C* 116: 9450–9460.

Slamet, Nasution, H.W., Purnama, E., Kosela, S. and Gunlazuardi, J. (2005). Photocatalytic Reduction of CO_2 on Copper-doped Titania Catalysts Prepared by Improved-impregnation Method. *Catal. Commun.* 6: 313–319.

Srinivas, B., Shubhamangala, B., Lalitha, K., Reddy, P.A.K., Kumari, V.D., Subrahmanyam, M. and De, B.R. (2011). Photocatalytic Reduction of CO_2 over Cu-TiO_2/Molecular Sieve 5A Composite. *Photochem. Photobiol.* 87: 995–1001.

Sutter, P., Acharya, D.P. and Camillone, N. (2011). CO_2

Adsorption, Diffusion, and Electron-Induced Chemistry on Rutile TiO_2(110): A Low-Temperature Scanning Tunneling Microscopy Study. *J. Phys. Chem. C* 115: 12095–12105.

Truong, Q.D., Liu, J.Y., Chung, C.C. and Ling, Y.C. (2012). Photocatalytic Reduction of CO_2 on $FeTiO_3/TiO_2$ Photocatalyst. *Catal. Commun.* 19: 85–89.

Tseng, I.H., Chang, W.C. and Wu, J.C.S. (2002). Photoreduction of CO_2 Using Sol-gel Derived Titania and Titania-supported Copper Catalysts. *Appl. Catal., B* 37: 37–48.

Tseng, I.H., Wu, J.C.S. and Chou, H.Y. (2004). Effects of Sol-gel Procedures on the Photocatalysis of Cu/TiO_2 in CO_2 Photoreduction. *J. Catal.* 221: 432–440.

Tu, W.G., Zhou, Y., Liu, Q., Tian, Z.P., Gao, J., Chen, X.Y., Zhang, H.T., Liu, J.G. and Zou, Z.G. (2012). Robust Hollow Spheres Consisting of Alternating Titania Nanosheets and Graphene Nanosheets with High Photocatalytic Activity for CO_2 Conversion into Renewable Fuels. *Adv. Funct. Mater.* 22: 1215–1221.

Ulagappan, N. and Frei, H. (2000). Mechanistic Study of CO_2 Photoreduction in Ti Silicalite Molecular Sieve by FT-IR Spectroscopy. *J. Phys. Chem. A* 104: 7834–7839.

Uner, D. and Oymak, M.M. (2012). On the Mechanism of Photocatalytic CO_2 Reduction with Water in the Gas Phase. *Catal. Today* 181: 82–88.

Varghese, O.K., Paulose, M., LaTempa, T.J. and Grimes, C.A. (2009). High-Rate Solar Photocatalytic Conversion of CO_2 and Water Vapor to Hydrocarbon Fuels. *Nano Lett.* 9: 731–737.

Wang, C.J., Thompson, R.L., Baltrus, J. and Matranga, C. (2010). Visible Light Photoreduction of CO_2 Using $CdSe/Pt/TiO_2$ Heterostructured Catalysts. *J. Phys. Chem. Lett.* 1: 48–53.

Wang, C.J., Thompson, R.L., Ohodnicki, P., Baltrus, J. and Matranga, C. (2011a). Size-dependent Photocatalytic Reduction of CO_2 with PbS Quantum Dot Sensitized TiO_2 Heterostructured Photocatalysts *J. Mater. Chem.* 21: 13452–13457.

Wang, P.Q., Bai, Y., Liu, J.Y., Fan, Z. and Hu, Y.Q. (2012a). One-pot Synthesis of Rutile TiO_2 Nanoparticle Modified Anatase TiO_2 Nanorods Toward Enhanced Photocatalytic Reduction of CO_2 into Hydrocarbon Fuels. *Catal. Commun.* 29: 185–188.

Wang, W.N., Park, J. and Biswas, P. (2011b). Rapid Synthesis of Nanostructured $Cu–TiO_2–SiO_2$ Composites for CO_2 Photoreduction by Evaporation Driven Self-assembly. *Catal. Sci. Technol.* 1: 593–600.

Wang, W.N., An, W.J., Ramalingam, B., Mukherjee, S., Niedzwiedzki, D.M., Gangopadhyay, S. and Biswas, P. (2012b). Size and Structure Matter: Enhanced CO_2 Photoreduction Efficiency by Size-Resolved Ultrafine Pt Nanoparticles on TiO_2 Single Crystals. *J. Am. Chem. Soc.* 134: 11276–11281.

Wu, J.C.S. and Huang, C. (2010). In Situ DRIFTS Study of Photocatalytic CO_2 Reduction under UV Irradiation. *Front. Chem. Eng. Chin.* 4: 120–126.

Xi, G.C., Ouyang, S.X. and Ye, J.H. (2011). General Synthesis of Hybrid TiO_2 Mesoporous "French Fries" Toward Improved Photocatalytic Conversion of CO_2 into Hydrocarbon Fuel: A Case of TiO_2/ZnO. *Chem. Eur. J.* 17: 9057–9061.

Xing, M., Fang, W., Nasir, M., Ma, Y., Zhang, J. and Anpo, M. (2013). Self-doped Ti^{3+}-enhanced TiO_2 Nanoparticles with a High-performance Photocatalysis *J. Catal.* 297: 236–243.

Xiong, L.B., Li, J.L., Yang, B. and Yu, Y. (2012). Ti^{3+} in the Surface of Titanium Dioxide: Generation, Properties and Photocatalytic Application. *J. Nanomater.* 2012: 1–13.

Yang, C.C., Mul, G., Yu, Y.H., Linden, B.V.D. and Wu, J.C.S. (2010). Artificial Photosynthesis over Crystalline TiO_2-Based Catalysts: Fact or Fiction? *J. Am. Chem. Soc.* 132: 8398–8406.

Yang, C.C., Vernimmen, J., Meynen, V., Cool, P. and Mul, G. (2011). Mechanistic Study of Hydrocarbon Formation in Photocatalytic CO_2 Reduction over Ti-SBA-15. *J. Catal.* 284: 1–8.

Yui, T., Kan, A., Saitoh, C., Koike, K., Ibusuki, T. and Ishitani, O. (2011). Photochemical Reduction of CO_2 Using TiO_2: Effects of Organic Adsorbates on TiO_2 and Deposition of Pd onto TiO_2. *ACS Appl. Mater. Interfaces* 3: 2594–6000.

Zhang, Q.Y., Li, Y., Ackerman, E.A., Gajdardziska-Josifovska, M. and Li, H.L. (2011). Visible Light Responsive Iodine-doped TiO_2 for Photocatalytic Reduction of CO_2 to Fuels. *Appl. Catal., A* 400: 195–202.

Zhang, Q.Y., Gao, T.T., Andino, J.M. and Li, Y. (2012). Copper and Iodine Co-modified TiO_2 Nanoparticles for Improved Activity of CO_2 Photoreduction with Water Vapor. *Appl. Catal., B* 123–124: 257–264.

Zhang, Y.H., Tang, Z.R., Fu, X.Z. and Xu, J. (2010). TiO_2-Graphene Nanocomposites for Gas-Phase Photocatalytic Degradation of Volatile Aromatic Pollutant: Is TiO_2-Graphene Truly Different from Other TiO_2-Carbon Composite Materials? *ACS Nano* 4: 7303–7314.

Zhao, B., Chen, F., Jiao, Y., Yang, H. and Zhang, J. (2012a). Ag-0-loaded Brookite/Anatase Composite with Enhanced Photocatalytic Performance Towards the Degradation of Methyl Orange. *J. Mol. Catal. A: Chem.* 348: 114–119.

Zhao, C.Y., Liu, L.J., Zhang, Q.Y., Wang, J. and Li, Y. (2012b). Photocatalytic Conversion of CO_2 and H_2O to Fuels by Nanostructured $Ce-TiO_2$/SBA-15 Composites. *Catal. Sci. Technol.* 2: 2558–2568.

Zhao, H.L., Liu, L.J., Andino, J.M. and Li, Y. (2013). Bicrystalline TiO_2 with Controllable Anatase–brookite Phase Content for Enhanced CO_2 Photoreduction to Fuels. *J. Mater. Chem. A* 1: 8209-8216, doi: 10.1039/c1033ta11226h.

Received for review, June 3, 2013
Accepted, July 11, 2013